Lin28b controls a neonatal to adult switch in B cell positive selection

Vanhee, Stijn; Åkerstrand, Hugo; Kristiansen, Trine Ahn; Datta, Sebak; Montano, Giorgia; Vergani, Stefano; Lang, Stefan; Ungerbäck, Jonas; Doyle, Alexander; Olsson, Karin; Beneventi, Giulia; Jensen, Christina T.; Bellodi, Cristian; Soneji, Shamit; Sigvardsson, Mikael; Gyllenbäck, Elin Jaensson; Yuan, Joan

Published in:
Science Immunology

DOI:
10.1126/sciimmunol.aax4453

2019

Document Version:
Peer reviewed version (aka post-print)

Lin28b controls a neonatal to adult switch in B cell positive selection

Stijn Vanhee[1], Hugo Åkerstrand[1], Trine Ahn Kristiansen[1], Sebak Datta[1], Giorgia Montano[1], Stefano Vergani[1], Stefan Lang[2], Jonas Ungerbäck[3], Alexander Doyle[1], Karin Olsson[1], Giulia Beneventi[4], Christina T Jensen[3], Cristian Bellodi[4], Shamit Soneji[2], Mikael Sigvardsson[3], Elin Jaensson Gyllenbäck[1], Joan Yuan[1]*

[1]Developmental Immunology Unit, Department of Molecular Hematology, Department of Laboratory Medicine, Lund Stem Cell Center, Lund University, Lund 22242, Sweden

[2]Computational Genomics Unit, Department of Molecular Hematology, Department of Laboratory Medicine, Lund Stem Cell Center, Lund University, Lund 22242, Sweden

[3]Molecular Lymphopoiesis Unit, Department of Molecular Hematology, Department of Laboratory Medicine, Lund Stem Cell Center, Lund University, Lund 22242, Sweden

[4]RNA and Stem Cell Biology Unit, Department of Molecular Hematology, Department of Laboratory Medicine, Lund Stem Cell Center, Lund University, Lund 22242, Sweden

*Correspondence: joan.yuan@med.lu.se.

One Sentence Summary: The temporally restricted expression of Lin28b augments neonatal B cell positive selection through amplifying the CD19/PI3K/c-Myc pathway, thereby potentiating the output of B-1 cells of self-reactive specificities early in life.

Summary

The ability of B-1 cells to become positively selected into the mature B cell pool, despite being weakly self-reactive, has puzzled the field since its initial discovery. Here, we explore changes in B cell positive selection as a function of developmental time by exploiting a link between CD5 surface levels and the natural occurrence of self-reactive B cell receptors (BCRs) in BCR wildtype mice. We show that the heterochronic RNA-binding protein Lin28b potentiates a neonatal mode of B cell selection characterized by enhanced overall positive selection and the developmental progression of $CD5^+$ immature B cells in particular. Importantly, Lin28b achieves this through amplifying the CD19/PI3K/c-Myc positive feedback loop and ectopic Lin28b expression restores both positive selection and mature B cell numbers in $CD19^{-/-}$ adult mice. Thus, the temporally restricted expression of *Lin28b* alters the rules for B cell selection during ontogeny through modulating tonic signaling. We propose that this neonatal mode of B cell selection represents a cell intrinsic cue to accelerate the de novo establishment of the adaptive immune system and incorporate a layer of natural antibody mediated immunity throughout life.

Introduction

Whereas T cell development relies on self peptide-MHC ligand mediated positive selection to effectively contribute to host defense (*1*), B cell function is not similarly constrained and adult immature B cells are purged for self-antigen reactivity even at low binding affinities (*2, 3*). Instead, developmental progression of newly formed immature B cells carrying innocuous BCRs rely on ligand independent tonic signaling mediated by the BCR and CD19 (*4-7*). Defying this censorship of self-reactivity are B-1 cells, an innate-like B cell subset harboring an oligoclonal and weakly self-reactive repertoire, that is excluded from germinal center reaction, and is responsible for a functionally distinct layer of antibody mediated immunity through the secretion of protective natural antibodies (*8*). Their positive selection was elegantly demonstrated using an anti-thymocyte autoantigen (ATAtg) specific BCR transgenic model, in which the presence of the Thy-1 self-antigen was a prerequisite for the establishment of transgene positive $CD5^+$ B-1 cells of this naturally occurring specificity (*9*). In the near two decades that followed this discovery, the basis for the ability of B-1 cells to escape central tolerance and undergo positive selection has remained unresolved.

Considering the predominant early life origin of $CD5^+$ B-1 cells, it is conceivable that B cell positive selection stringency may be temporally controlled during ontogeny. Indeed, transgenic

expression of BCRs directed against self-antigens such as phosphatidylcholine (PtC) are efficiently incorporated into the neonatal B cell repertoire while being excluded in favor of endogenous BCRs in the adult (*9-12*). However, although the use of BCR transgenic models has been instrumental in unveiling unique aspects of B-1 cell selection, conclusions were limited to a few B-1 restricted antigen specificities in a non-physiological setting. To date, the underlying molecular mechanisms for such a putative ontogenic switch in B cell selection remain unknown.

Lin28b is a mammalian paralog of the heterochronic RNA binding protein Lin28, first described in *C. elegans* to block the biogenesis of the let-7 family of microRNAs and thereby control the timing of developmental events (*13*). We have previously shown that Lin28b exhibits a fetal restricted expression pattern during murine hematopoiesis and that ectopic expression in the adult promotes key aspects of fetal-like lymphopoiesis including the efficient production of $CD5^+$ B-1 cells (*14, 15*). Since then, additional evidence from the lymphoid, erythroid, and megakaryocyte lineages have cemented the role of Lin28b as a multi-lineage molecular switch for fetal hematopoiesis (*16-20*). However, the requirement for endogenous Lin28b during early life B lymphopoiesis has not been explored.

CD5 is a negative regulator of antigen receptor signaling and was first identified as a surface molecule expressed on human T cells and B chronic lymphoblastic leukemia cells (*21*). Parallel observations in mice and men established a positive correlation between the frequency of $CD5^+$ B cells and antibody polyreactivity (*22*). More recently, it was shown in antigen receptor transgenic mice that CD5 levels reflect the degree of self-antigen reactivity in T and B cells (*9, 23-26*). In this study, we use surface CD5 levels to interrogate ontogenic changes in B cell positive selection in BCR wildtype (WT) mice. Our results demonstrate that B cell positive selection is temporally controlled during ontogeny by endogenous *Lin28b* through amplifying a previously reported positive feedback loop involving CD19 and c-Myc (*27-29*). Thus, Lin28b acts as a cell intrinsic enhancer of overall immature B cell positive selection, including the efficient developmental progression of weakly self-reactive B-1 cells early in life.

RESULTS

Establishing a positive correlation between CD5 expression and self-reactivity in BCR wildtype B-1 cells

The murine adult B-1 cell compartment displays a range of CD5 surface levels, with those originating from fetal liver (FL) hematopoietic stem and progenitor cells (HSPCs) displaying the most surface expression. While B-1 cells can mature in low numbers from adult HSPCs (*30-32*), these exhibit markedly lower surface CD5 expression (Figure 1A)(*33*). Thus, we reasoned that uncovering the significance and developmental control of B cell CD5 levels would be critical in understanding the ontogenic switch in B cell output leading to reduced B-1 cell generation. While CD5 expression has been linked to self-reactivity in BCR transgenic mouse models, this link has not been empirically established in a non-transgenic BCR setting. To this end, we took advantage of the high degree of self-antigen driven clonal dominance in the B-1 compartment as a measure of self-reactivity and analyzed the BCR repertoires of sorted $CD5^{hi}$, $CD5^{int}$, $CD5^{low}$ and $CD5^{neg}$ peritoneal cavity B-1 cells from WT adult C57BL/6 mice (Figure 1B). The successful separation based on amount of CD5 surface expression was confirmed by FACS analysis (Figure 1C) and subsequent IgHM BCR repertoire sequencing analysis (VDJseq) demonstrated a clear correlation between increasing CD5 expression and CDR3 clonal dominance (Figure 1D). This was quantified by the inequality index (Gini coefficient) of clonal representation (Figure 1E). In addition, we observed a gradual increase in the representation of IGHV-11 and IGHV-12 gene segment usage, known to primarily encode the self-reactive specificity against PtC, with rising CD5 levels (Figure 1F). This observation is consistent with FACS data displaying increasing PtC liposome reactivity (Figure 1G). Consistent with the superior ability of fetal HSPCs to generate $CD5^{+}$ B-1 cells (Figure 1A) and the lack of TdT expression during fetal life (*34*), the presence of N-nucleotide additions inversely correlated with CD5 levels (Figure 1H). These data establish that surface CD5 expression correlates with B cell self-reactivity and early ontogeny in a BCR WT setting, providing a practical readout for self-reactivity in a non-BCRtg setting.

Lin28b potentiates an elevated mode of positive selection unique to neonatal mice

During adult B cell development in WT mice at steady-state, CD5 expression is restricted to self-reactive transitional B cells in the spleen doomed for anergy and exclusion from the long-

lived B cell pool (*25*). This is in contrast to the T cell lineage, where reactivity towards self-peptide-MHC complex is a desirable feature and CD5 is developmentally induced during positive selection in the $CD4^+CD8^+$ double positive thymocyte stage (*23, 24*). Considering that $CD5^+$ B-1 cells are allowed to mature early in life, we hypothesized that neonatal self-reactive $CD5^+$ immature B cells would be positively selected into the mature B cell pool, analogous to $CD4^+CD8^+$ double positive thymocytes, rather than being purged from the naïve B cell repertoire. In line with this hypothesis, we found that both the median fluorescence intensity (MFI) and the spread in surface CD5 levels as measured by interquartile range (IQR) were significantly elevated as neonatal bone marrow (NBM) pre-B cells entered the IgM^+CD93^+ immature B cell stage (Figures 2A, S1A). Notably, this emergence of $CD5^{hi}$ cells was apparent in the neonate but not adult immature B cells and coincides with the timing of central tolerance establishment (*35*). Although only present at low frequencies ($0.45\% \pm 0.25\%$) among neonatal immature B cells, PtC reactive cells reside within this $CD5^{hi}$ fraction (Figure 2B), suggesting that CD5 levels are induced during B cell maturation on the basis of self-reactivity. The neonatal specific expression of CD5 on immature B cells was mirrored by the presence of $CD5^+$ transitional T1 cells in the neonatal but not adult spleen (Figure S1B) known to be destined for the B-1 lineage (*36*). Considering the link between CD5 expression and BCR self-reactivity, these results are consistent with an increase in the tolerated spectrum of self-reactive specificities and an age restricted licensing of an enhanced mode of positive selection in neonatal immature B cells.

We and others have previously established Lin28b as a molecular switch capable of reinitiating fetal-like hematopoiesis including B-1 cell output (*14, 15, 20*). However, these data were exclusively based on ectopic expression of either Lin28a or Lin28b. To investigate whether endogenous Lin28b is required for the maturation of $CD5^+$ B-1 cells during neonatal life, we analyzed *Lin28b*$^{-/-}$ neonatal mice (*37*). We found that Lin28b deficiency led to decreased CD5 MFI and IQR in the immature B compartment in a dose dependent manner (Figure 2C), resulting in the subsequent reduction in the percentage of $CD5^+$ transitional T1 B cells in the spleen (Figure S1C) and mature B-1 cell output in the peritoneal cavity (Figure 2D-E). These data suggest that permissiveness towards $CD5^+$ immature B cells and developmental progression of $CD5^+$ B-1 cells relies on endogenous Lin28b in neonatal mice. In line with this notion, we observed a postnatal decline in immature B cell surface CD5 levels that coincides with the timing of the attenuation in Lin28b mRNA expression in hematopoietic stem cells (HSCs) (*15*) and becomes indistinguishable from the levels in adult immature B cells by day

19 of age (Figure 2F). Furthermore, we observed a positive correlation between increased Lin28b dosage and immature B cell size as measured by forward scatter (Figure 2G); a hallmark of B cell positive selection (*6*). We conclude that Lin28b expression early in life potentiates an elevated mode of positive selection characterized by the tolerance of CD5+ immature B cells and the output of $CD5^+$ B-1 cells during the first weeks of life.

Ectopic expression of Lin28b is sufficient to augment overall B cell positive selection in adult mice

To address whether ectopic Lin28b expression during adult B cell maturation is sufficient for potentiating the generation of $CD5^+$ immature B cells we put tet-Lin28b mice (*38*) on a doxycycline (DOX) diet for a minimum of 10 days. Lin28b transgene expression resulted in a potent increase in CD5 MFI and IQR upon pre-B to immature B cell transition (Figure 3A). Increased CD5 levels were accompanied by a tet-Lin28b induced increase in immature B cell size (Figure 3B) and the emergence of $CD5^+$ transitional T1 cells in the spleen (Figure S1D), consistent with the neonatal mode of enhanced positive selection (*6, 36*). Despite the observed increase in cell size, we did not observe apparent changes in the percentage of replicating cells among tet-Lin28b pre-B and immature B cells (Figure S2A-D) consistent with an modest increase in cellular anabolism. Next, we performed adoptive transfer experiments of the 20% highest and lowest CD5 expressing immature B cells from DOX treated tet-Lin28b mice into individual non-DOX treated Rag1KO recipients to track the maintenance of CD5 expression in the periphery. Three weeks post adoptive transfer, CD5 levels were largely maintained in most donor derived mature B cells demonstrating that $CD5^+$ immature B cells are predisposed to give rise to $CD5^+$ B-1 cells in a cell intrinsic manner (Figure 3C-E). Furthermore, PtC reactive specificities exclusively derived from the $CD5^+$ donor population (Figure 3F), consistent with CD5 marking self-reactive immature B cells.

To establish at which stage during B cell development Lin28b is required to mediate efficient $CD5^+$ B-1 cell output, we adoptively transferred either pro-B, pre-B or immature B cells from untreated tet-Lin28b donor mice into DOX fed RAG1KO recipients (Figure S3A). $CD5^+$ B-1 cell output was most efficient when transgene expression is initiated at the pro-B cell stage, and declines when initiated later at the pre-B and immature B stages (Figure S3B). We subsequently performed the reverse experiment in which tet-Lin28b transgene expression in DOX treated donor mice was turned off at different stages of B cell differentiation upon adoptive transfer

into untreated RAG1KO recipients. Our results demonstrate that cessation of Lin28b transgene expression before the immature B stage is detrimental to developmental progression of progenitors destined for the $CD5^+$ B-1 fate (Figure S3B). Although there is a delay in transgene expression / cessation post transfer, these data firmly establish a need for Lin28b expression during the central tolerance checkpoint of B cell maturation (Figure S3C).

To quantitatively test whether the efficiency of B cell positive selection is enhanced by Lin28b, we measured mature B cell output by single cell lineage tracing of pre-selection pro-B cells using lentiviral cellular barcoding (*15, 39*). Pro-B cells were FACS sorted from the ABM of uninduced tet-Lin28b mice and transduced with a lentiviral library (Barcode-GFP-LV) encoding high complexity DNA barcodes (*40*) (Figure 4A). Following transduction, the cells were divided into two equal halves that were adoptively transferred into Rag1KO recipients fed with either DOX or normal diet respectively. GFP^+ mature B cells were isolated from the recipient spleen two weeks post transfer and analyzed for unique barcode content as a measure of relative selection efficiency (Figure S4A-E). The number of unique progenitors that contributed to mature B cells was significantly increased upon ectopic Lin28b expression (Figure 4B-C). Barcode read frequency analysis did not reveal any unbalanced clonal expansion over the course of the experiment (Figure 4B). Since barcode labelling efficiency was directly comparable, our finding is consistent with an increase in progeny:precursor ratio and thereby selection efficiency. In addition, both splenic mature B-1 and follicular B-2 cells from DOX treated recipients displayed increased CD5 levels (Figure 4D-E). These data are reminiscent of previous observations that the majority of B cells in the human fetal spleen and cord blood are $CD5^+$ (*41-43*) and implicate Lin28b in the mechanism underlying this developmentally restricted expression pattern. We conclude that Lin28b augments overall B cell positive selection including selection into the B-1 lineage.

To track the kinetics of developmental progression through the central tolerance checkpoint in the presence or absence of Lin28b expression *in vivo*, we pulsed DOX induced tet-Lin28b and WT mice with a single dose of EdU and assessed labeled B cells after 2, 24, 48, 72 and 96 hours of chase. Interestingly, while initial labelling efficiency of IgM^- ABM B cell progenitors from tet-Lin28b and WT mice were comparable, labelled tet-Lin28b cells displayed accelerated progression through the ABM B cell stages and emergence into the splenic transitional T1 stage (Figure 4F-H). Taken together, our data demonstrates that Lin28b promotes overall positive

selection efficiency leading to accelerated developmental progression of bone marrow immature B cells.

Lin28b promotes B cell positive selection through amplifying the CD19/PI3K/c-Myc feedback loop

To explore the molecular pathway by which Lin28b regulates B cell positive selection we performed RNAseq analysis of tet-Lin28b induced and WT ABM immature B cells. Differential gene expression analysis identified an increase in the expression of several previously known Lin28b/let-7 target genes (e.g. *Igf2bp3*, *Myc* and *Lin28b* itself) (Figure 5A) as well as increased *Cd5* and *Nr4a1* (Nur77) transcript levels (Figure 5B) consistent with enhanced self-reactivity (Figure 3)(*44*). Unsupervised Gene-set enrichment analysis (GSEA) of the hallmark gene set collection from the Molecular Signature Database (*45*) identified c-Myc induced targets as the top upregulated molecular signature upon tet-Lin28b transgene expression (Figure 5C and S5). let-7 and interferon gamma response target genes served as positive and negative controls of our GSEA analyses respectively. In line with this, we observed a consistent increase in *Myc* mRNA and protein levels upon ectopic tet-Lin28b expression in ABM immature B cells (Figure 5E-F). This finding is consistent with previous reports establishing c-Myc as a let-7 target that is derepressed upon Lin28b expression (*46, 47*).

Next, to assess whether c-Myc protein levels are controlled by endogenous Lin28b during neonatal B cell maturation we performed intracellular FACS staining (Figure 5G). Interestingly, we observed an elevated level of c-Myc protein in WT neonatal immature B cells compared to their adult counterparts. This elevated c-Myc expression is decreased in in neonatal Lin28b$^{-/+}$ and Lin28b$^{-/-}$ immature B cells in a dose dependent fashion. The same trend was observed by immunoblotting of total neonatal splenic lysates from the same genotypes (Figure 5H). In line with this finding, RNAseq analyses of sorted neonatal immature B cells revealed a depletion of c-Myc target genes among Lin28b$^{-/-}$ mice (Figure 5I). Thus, Lin28b critically maintains an elevated level of c-Myc protein levels and function during neonatal B cell maturation.

To assess whether transgenic c-Myc overexpression mediates increased positive selection of immature B cells we analyzed pre-cancerous Eu-Myc transgenic mice. Our findings demonstrate decreased lambda light chain usage (Figure S6A-B), increased cell size (Figure S6C) and a trend, although not significant, towards increased surface CD5 expression (Figure

S6D-E) consistent with increased positive selection and a partial recapitulation of tet-Lin28b induced B cell maturation. We also observed a marked increase in CD19 surface expression on Eu-Myc immature B cells consistent with the previously reported CD19/c-Myc positive feedback loop (Figure S6F) (*28*). We did not, however, detect any reactivation of endogenous *Lin28b* expression as has been shown in several human and murine tumor models (Figure S6G-H)(*48, 49*). Taken together, our evidence suggests that c-Myc is an important mediator of Lin28b mediated positive selection. It is important to note that c-Myc is not the only downstream mediator of Lin28b. We observed several other significantly enriched molecular signatures in our GSEA analysis (Figure 5C and S5) including E2F, oxidative phosphorylation and MTORC1 signaling consistent with previous reports of Lin28b action (*38, 47, 50*).

Previous studies have implicated c-Myc as a key mediator of the CD19/PI3K signaling pathway which critically controlls immature B cell positive selection and mature B cell survival (*27-29, 51-53*). CD19$^{-/-}$ mice display reduced c-Myc protein levels (*28*) extensive receptor editing and developmental arrest of immature B cells (*5-7*) as well as decreased peripheral B cell numbers and B-1 cell representation (*54-56*). We crossed the tet-Lin28b transgene onto a *CD19*$^{-/-}$ background (*55*) to test whether Lin28b induced Myc expression can genetically rescue the observed defects i *CD19*$^{-/-}$ mice. Following a 3-week-DOX treatment, we observed a near complete rescue of splenic B cell numbers in tet-Lin28b transgenic *CD19*$^{-/-}$ mice (Figure 6A-B) as well as a partial rescue of B-1 cell representation (Figures S6I-K). FACS analysis of *CD19*$^{-/-}$ immature B cells revealed the expected characteristics of impaired positive selection including decreased CD5 levels, enhanced lambda : kappa light chain usage ratio (Figure 6C-E) and reduced immature B cell representation (Figure S6L). These defects were also restored to normal adult levels by tet-Lin28b expression. These results demonstrate a potent ability of Lin28b to functionally compensate for CD19 during B cell selection and maintenance.

To assess whether tet-Lin28b expression restores c-Myc expression in CD19$^{-/-}$ mice we performed western blot analyses. Indeed, c-Myc protein in total splenic B cells were restored by tet-Lin28b transgene expression. In addition, Lin28b also restored PI3K pathway defects observed in CD19$^{-/-}$ mice as measured by phospho-PDK1, and GSK3b, and phospho-S6 (Figure 6F-G), consistent with a previously reported role for Lin28b in the positive regulation of the PI3K/MTORC1 signaling pathway (*38*) as well as our own RNAseq analyses (Figure 5C). We conclude that Lin28b promotes B cell positive selection at least in part through the amplification of a previously reported c-Myc / PI3K positive feedback loop (*27-29*).

Lin28b induced positive selection in the adult produces fully functional CD5$^+$ B-1 cells

To assess the functionality of CD5$^+$ B-1 cells induced by tet-Lin28b mediated positive selection in the adult, we compared their *in vivo* and *in vitro* effector functions to natural CD5$^+$ B-1 cells found in unperturbed adult WT mice ($_n$B-1). To this end, we first established a transplantation-based model system that circumvents a critical pitfall of previous approaches (*14, 20*) in which constitutive overexpression of Lin28A/B in mature B-1 cells failed to resolve developmental effects on positive selection from those on mature B-1 cell maintenance and function. Donor tet-Lin28b ABM HSPCs were DOX treated for 4 weeks to allow for a transient wave of fetal-like CD5$^+$ B-1 cell ($_{L28}$B-1) output upon transfer into pre-conditioned RAG1KO recipient mice (Figure 7A). WT FL and ABM LSK HSPCs were similarly transplanted yielding $_{FL}$B-1 and $_{ABM}$B-1 control populations respectively. Donor derived B-1 cells were analyzed following a 12-week chase period during which DOX treatment was removed. We confirmed the cessation of ectopic Lin28b protein expression and the subsequent decline of ongoing B-1 maturation (Figure S7A-B), which mimics the natural down-regulation of endogenous *Lin28b* during postnatal life (*14, 17*). While WT ABM HSPCs produced a low frequency of CD5$^+$ B-1 cells, transient Lin28b expression resulted in the long-term reconstitution of $_{L28}$B-1 cells with a similar CD5 expression profile as $_n$B-1 cells (Figure 7B-C and S7C-E). To more rigorously assess the long-term survival of $_{L28}$B-1 cells in the absence of ABM influx, a hallmark of B-1 cell biology (*57*), we performed competitive transfer of FACS sorted test B-1 cell subsets at a 1:2 ratio with $_n$B-1 congenic competitor cells into Rag1KO mice. At 12 weeks post transfer, the $_{L28}$B-1 cells displayed long-term fitness comparable to $_{FL}$B-1 cells and $_n$B-1 cells (Figure 7D). In contrast, $_{ABM}$B-1 cells were markedly outnumbered by competitor cells. Thus, continuous Lin28b expression is not required for the bone marrow independent long-term maintenance of $_{L28}$B-1 cells in the periphery. Instead, our data suggests that the initial Lin28b dependent mode of B-1 cell selection is the main predictive parameter of longevity. Interestingly, the stability of surface CD5 levels closely mirrored our observations of peripheral maintenance. While $_{L28}$B-1 cells maintained their CD5 levels long-term, the remaining $_{ABM}$B-1 cells, initially sorted for CD5 positivity, displayed a lower CD5 expression profile at the time of analysis (Figure 7E). Corroborating this data, CD5 levels on $_{ABM}$B-1 cells were destabilized upon *in vitro* LPS stimulation but remained constant on $_{L28}$B-1 and $_n$B-1 cells (Figure S7F). We conclude that the long-term fitness and stability in CD5 expression critically depend on the Lin28b mediated mode of positive selection.

One hallmark of B-1 cells is their semi-invariant repertoire stemming from the lack of TdT expression early in life (*34*). To address the diversity of the $_{L28}$B-1 BCR repertoire, we performed VDJseq of the immunoglobulin heavy chain repertoire. Our results demonstrate that $_{L28}$B-1 cells, like $_{ABM}$B-1 cells exhibit high junctional diversity (Figure 7F). These results are in line with the observation that Lin28b does not abrogate TdT expression in ABM pro-B cells (Figure S5G) and is consistent with a previous report based on constitutive Lin28b overexpression (*20*). Thus, we conclude that Lin28b allows for the positive selection of a highly diverse repertoire of $CD5^+$ immature B cells and that germline encoded specificities prevalently employed early in life are not a prerequisite for neonatal-like B cell positive selection or long-lived B-1 cell fate.

Finally, we assessed IgM and IL-10 secretion as two important B-1 effector functions. Our results show that both $_{L28}$B-1 and $_{ABM}$B-1 isolated from the spleen cells are capable of spontaneous IgM secretion by ELISPOT assay. Furthermore, IL-10 production upon in vitro LPS stimulation of both $_{L28}$B-1 and $_{ABM}$B-1 was comparable to $_{n}$B-1 and $_{FL}$B-1 levels (Figure 7G-H). We conclude that Lin28b dependent positive selection produces functionally competent B-1 cells and is a prerequisite for the B-1 signature characteristics of long-term survival and stable CD5 expression. However, the Lin28b dependent mode of positive selection is not required for other critical innate-like functional properties such as IL-10 production and spontaneous IgM secretion (*8*) (Figure 7I).

DISCUSSION

In this study, we demonstrate that the early life restricted expression pattern of Lin28b potentiates an enhanced mode of B cell positive selection during a limited window of time. Numerous studies have previously cemented a role for Lin28b as a multilineage master regulator of fetal like hematopoiesis (*14, 16-20*). Our finding that Lin28b promotes positive selection through amplifying a positive feedback loop involving CD19 and c-Myc represents a highly B lineage specific mode of Lin28b action. CD19 overexpression has previously been demonstrated to enhance positive selection, B-1 cell numbers as well as autoantibody production by shifting the selection criteria for newly formed B cells (*54, 58, 59*). Thus, the ability of Lin28b to replace CD19 mediated tonic signaling during B cell maturation represents a cell intrinsic mechanism of altering the threshold for B cell selection early in life and position

the Lin28b/let-7 axis among a growing list of miRNA dependent modes to fine-tune the PI3K pathway and B cell selection (*29, 60, 61*).

Our results suggest that the proto-oncogene c-Myc, which promotes B lymphomagenesis through the CD19/PI3K pathway (*28, 62*), is one mediator of Lin28b action in B cells. In addition to being a let-7 target that is derepressed upon Lin28 expression (*46-48, 63*) the *Myc* transcript was recently found to be bound by Lin28b which may result in stabilization of the transcript (*64*). These findings are consistent with a conserved functional synergy between Lin28b, itself a c-Myc transcriptional target, and c-Myc during normal development, induced pluripotent stem cell reprogramming as well as oncogenic transformation. Previously, another let-7 target, Arid3a, was shown to be ontogenically controlled by Lin28b (*20*), and to promote B-1 cell output in part through upregulation of Myc expression (*65*). These findings implicate Arid3a as an additional player in the molecular network controlling the neonatal mode of positive selection. Many questions remain as to how Lin28b achieves enhanced B cell positive selection including to what extent death by neglect and negative selection is suppressed and how Lin28b deploys let-7 dependent versus independent mechanisms. Importantly, Lin28b (*66*) and CD5 (*67*) positive subtypes of pediatric acute lymphoblastic leukemias have been independently described and highlight the need to dissect whether or not endogenous Lin28b is complicit with c-Myc in the oncogenesis of B cell cancers.

Previously, the topic of B-1 cell selection has mainly been studied through the narrow lens of a small number of germline encoded BCR specificities using BCR transgenic mice. Here, we use several innovative approaches to tackle this question in BCR WT mice. First, we establish CD5 FACS analysis as a useful tool for studying immature B cell positive selection in general, and neonatal mice in particular. Second, our use of cellular barcoding represents a suitable method for quantifying the relative precursor-progeny frequency of B cell selection efficiency that circumvents confounding parameters of VDJseq based approaches such as receptor editing. Third, our use of transient tet-Lin28b induction in a transplantation setting allowed us to tease apart transgene effects on B cell positive selection from those on mature B cell function and maintenance. Together, these approaches have allowed us to demonstrate that Lin28b expression during the central tolerance check-point is necessary and sufficient for the generation of fully functional long-lived B-1 cells on the backdrop of a highly diverse adult type BCR repertoire. Although the degree and specificity of self-antigen reactivity of tet-Lin28b induced $CD5^+$ B-1 cells that are not PtC reactive remain to be empirically determined, our

findings indicate that the Lin28b dependent mode of B-1 cell selection into the mature B cell pool is a predictive feature of bone marrow independent self-renewal.

Despite the many remaining questions, our study establishes an undeniable link between developmental timing and B cell signaling strength. This is a significant advancement in our understanding of B-1 cell fate determination that reconciles two compelling yet previously disjointed bodies of work emphasizing the importance of early progenitor ontogeny on the one hand (*68-70*) and BCR driven events on the other (*21, 71-74*). Most recently, elegant work from Graf et al (*74*) demonstrating that the Cre recombinase mediated exchange of BCR transgene identity in mature naïve follicular B-2 cells confer B-1 functionality cemented the instructive power of BCR signaling. However, CD5 expression was not fully restored in these BCR switched cells leaving open the possibility that additional developmental determinants are required for complete reprogramming to natural B-1 fate (*74*). To this end, our finding that CD5 levels are set in the immature B cell stage and that transient Lin28b expression during, but not beyond, bone marrow B cell selection is a requirement for stably maintained CD5 expression provides the missing link. Importantly, our findings represent a mechanistic explanation to the early life bias of $CD5^+$ B-1 cell output providing a unified model for B-1 lineage choice in which Lin28b acts as a developmentally restricted regulator of B cell signaling, which in turn instructs B-1 cell fate during positive selection.

The risks for incorporating harmful auto-reactivity raises the stakes for Lin28b dependent enhancement of positive selection early in life. Still, when restricted to a narrow developmental window during ontogeny, this seemingly reckless behavior may confer significant evolutionary gains for the host. First, this may represent a critical mechanism to accelerate the expansion phase of the adaptive immune system during the sensitive neonatal period to mitigate the potential risks of lymphopenia. Second, it represents an opportunity for the incorporation of useful poly-reactive, and by definition somewhat self-reactive, specificities into the mature B cell pool that could contribute to tissue homeostasis as well as close any gaps in our immune system exploitable by pathogens. Moreover, continuous encounter of self-antigen primes innate-like B cells for rapid and intense responses prior to the delayed response of conventional follicular B-2 cells. Given that the lack of TdT expression severely restricts CDR3 diversity early in life, the benefits of Lin28b dependent positive selection may outweigh the limited risks for generating harmful autoimmunity. Indeed, the unique role of polyreactive antibodies in humoral immunity is widely recognized in both the broad antimicrobial function of natural

antibodies as well as the highly specific protection responses to thymus dependent antigens (*75, 76*). Taken together, our work provides key insights into the phenomenon of B cell positive selection from a developmental biology perspective and highlights the contribution of the ontogenically restricted expression pattern of Lin28b to the establishment of peripheral B cell heterogeneity and life-long antibody diversity.

Methods

Mice

Col1a1tm2$^{tetO\text{-}LIN28B}$ mice crossed to R26m2rtTA were obtained from the laboratory of Dr. George Daley (*38*) (Harvard Medical School). Transheterozygous mice are herein referred to as tet-Lin28b. In all experiments where tet-Lin28b mice were used, control mice harboring the R26m2rtTA allele was used and is designated as "WT" in the figures. The following mouse strains were obtained from the Jackson Laboratory. Lin28b$^{-/-}$ (B6.Cg-*Lin28b*$^{tm1.1Gqda}$/J strain nr. 023917) (*37*). Rag1KO (B6.129S7-*Rag1*^{tm1Mom}/J strain nr. 002216). CD45.1 (B6.SJL-*Ptprc*^{a} *Pepc*^{b}/BoyJ strain nr. 002014). CD19 heterozygous mice (B6.129P2(C)-*Cd19*$^{tm1(cre)Cgn}$/J strain nr. 006785) EuMYC mice (B6.Cg-Tg(IghMyc)22Bri/J strain nr. 002728). Adult mice were 10 - 16 weeks of age and unless specified differently, neonatal mice were 2-3 days of age. For experiments where CD45.1+CD45.2+ congenic mice were used CD45.1 (B6.SJL) were intercrossed with CD45.2 (B6NTac, Taconic). All animal procedures were performed in accordance with ethical permits approved by the Swedish Board of Agriculture.

For HSPC transplantations, Lineage^{-}(Lin^{-}: Ter119^{-}B220^{-}Gr1^{-}CD3e^{-}) Sca1^{+}cKit^{+} HSPCs (LSK) cells from E14.5 FL, or Lineage^{-}(Lin^{-}: Ter119^{-}B220^{-}Gr1^{-}CD11b^{-}CD3e^{-}) Sca1^{+}cKit^{+} HSPCs (LSK) cells ABM were harvested from indicated donor mice. The equivalence of 10 000 sorted CD45.2^{+}CD45.1^{+} double-positive LSKs were transplanted into either Rag1KO or into congenic CD45.1 recipient mice together with 200 000 CD45.2 total BM support cells. Recipient mice were irradiated (1x 450cGy for Rag1KO and 2 × 450 cGy for CD45.1) and transplanted by intravenous (I.V.) tail vein injection. All mice were given 125mg/L ciproxin containing water for 2 weeks following irradiation. Donor reconstitution was assessed by peripheral blood analysis 6-8 weeks after transplantation. Endpoint analysis was performed 16–20 weeks after transplantation as indicated for each experiment. For the DOX-STOP regimen, recipient mice were fed DOX diet (200+ mg/kg DOX, Sniff GMBH) for 7 days prior to transplantation with indicated donor cells and 4 weeks after transplantation. Mice were analyzed after a DOX free chase period of 12 weeks.

For competitive adoptive transfer experiments of peritoneal cavity CD5^{+}B-1 cells, 20 000 CD45.2^{+} donor cells from primary recipients were mixed at a 1:2 ratio with CD45.1^{+} or

CD45.1$^+$CD45.2$^+$ congenic CD5$^+$B-1 cells competitor cells and injected intraperitoneally (I.P) into Rag1KO recipients.

Lentiviral cellular barcoding and transplantation of pro-B cells

100 000 pro-B cells defined as Lin$^-$(Ter119$^-$ CD11b$^-$ Gr1$^-$ CD3e$^-$) CD19$^+$ B220$^+$ IgM$^-$ CD93$^+$ cKit$^+$ CD43$^+$ CD24^{lo}CD25$^-$ were sorted and transduced with Barcode-GFP-LV (*40*) as previously described (*15*). The equivalence of 50 000 sorted and transduced pro-B cells were transplanted per RAG1KO recipient 12h following Barcode-GFP-LV transduction. Recipients for cells in the +DOX condition were maintained on a Dox diet starting 7 days prior to transplantation and throughout the course of the experiment. Splenic mature B cells (CD19$^+$CD93$^-$GFP$^+$) were FACS sorted 2 weeks following transplantation and analyzed for barcode content as previously described (*15*). Samples were indexed using Nextera XT indexing kit (Illumina) and sequenced using the Illumina NextSeq platform (Illumina). Two technical PCR replicates were performed from the genomic DNA of each population and only barcodes found in both technical replicates were considered for analysis.

Flow Cytometry

Antibodies are detailed in Table S1. BM cells were extracted by crushing the bones from hind limbs, hips, and spine with mortar and pestle (*77*). BM and spleens were subjected to red blood cell lysis. For pro-B cell or immature B cell isolation, total BM cells were pre-enriched by MACS (Miltenyi Biotec) depletion of Lineage$^+$ cells (Ter119$^+$Gr1$^+$CD11b$^+$CD3e$^+$) according to manufacturer's instructions prior to FACS sorting. Peritoneal lavage was performed using 10 mL (adult) or 2 mL (10-day neonate) FACS buffer (HBSS, GIBCO) supplemented with 0.5% BSA and 2 mM EDTA. Antibody staining was performed in FACS buffer at a density of maximum 1x10^7 cells/100uL volume for 30 min on ice. All FACS experiments were performed at the Lund Stem Cell Center FACS Core Facility, Lund University, on FACS Aria III, FACS Aria IIu, Fortessa and LSRII instruments (Becton Dickinson). Bulk populations were sorted using a 70-micron or 85-micron nozzle, 0.32.0 precision mask, and a flow rate of maximally 6000 events/second. For intracellular staining, a maximum of 10x10^6 cells were fixed in 100uL 4% formaldehyde at room temperature for 15 minutes. After washing in FACS buffer, cells were permeabilized in 0,5% Triton-X in PBS at room temperature for 15 minutes prior to washing and staining.

VDJSeq

VDJSeq was performed as previously described (*78*). All analyses were performed using R version 3.2.1 (2015) and R version 3.5.2 (2018) (R Core Team, URL http://www.R-project.org/.). Circos plots were generated using the R Circlize package v0.4.5 (*79*) Gini indexes were calculated using the R Reldist package 1.6-6. R scripts are available upon request.

EDU pulse label

Mice were injected intraperitoneally with a single dose of 5mg EDU (5-Ethynyl-2'-deoxyuridine, Abcam). At the indicated time points, $10x10^6$ total bone marrow or spleen cells were prepared and stained for surface markers as described above. Next, cells were fixed in 4% paraformaldehyde for 15 minutes at room temperature and permeabilized using a solution of 0,5% Triton-X in PBS for 15 minutes at room temperature. Subsequently, the Click-It reaction between EDU and azide-AlexaFluor555 was performed according to the manufacturers protocol (Thermo Scientific).

Ki67 labeling

10x10e6 total bone marrow cells were prepared and stained for surface markers as described above. Next, cells were fixed and permeabilized using the Transcription Factor Buffer Set (BD pharmingen) according to the manufacturers instructions. Cells were stained with anti-Ki67 antibody (BD biosciences) and appropriate isotype control. Before acquisition cells were incubated with 1ug/ml DAPI for 30' at RT.

ELISpot

plates were pre-wet with 35% ethanol and washed 3-4 times with sterile PBS before coating the plate with a-IgM (8ug/ml). Plates were coated O/N at 4°C. After washing with PBS, wells were blocked with 3% BSA in PBS for 2h at RT. After washing, 20.000 cells were plated in culture medium and incubated overnight at 37°C. For detection of spots, wells were washed with 0,05% Tween-20 in PBS. After washing with PBS, a-IgM-HRP was added and incubated for 1.45h at RT. After washing with PBS, TMB solution was added for 8 minutes. Plates were then washed with distilled water and dried before spot counting.

ELISA

ELISA plates were coated with a IL-10 antibody in carbonate buffer (0.1M Na_2CO_3: 0.1 M $NaHCO_3$ pH=9.6 at a 1:3 ratio) overnight at 4°C. Plates were washed with PBS-T (PBS with 0.1% Tween 20) and blocked with 1% BSA in PBS and incubated at RT for 2h. After washing

with PBS-T plates were washed before adding appropriate sample dilutions. After washing with PBS-T and anti-IgM-HRP antibody was added for 2h at RT. After washing of plates with PBS-T, TMB substrate (Pierce) was added. The reaction was stopped by carefully adding an equal amount of STOP solution (2M H_2SO_4) to the TMB substrate.

RNAseq

RNAseq was performed on sorted immature B cells ($CD19^+B220^{lo}CD93^+IgM^+CD24^{hi}$) from tet-Lin28b or WT mice fed DOX food for 2 weeks; or 3d old neonatal Lin28b wild-type, heterozygous or knockout mice . Libraries were generated using the Smartseq V4 Ultra Low input RNA Library Prep Kit (Clontech) and the Nextera XT DNA indexing kit (Illumina) according to the manufacturer's instructions. Libraries were indexed using the Nextera XT v2 indexing kit (Illumina) according to the manufacturers instructions. Libraries were sequenced on an Illumina Nextseq system using a Nextseq V500/550 150cycle high output kit. Reads were aligned using STAR aligner v2.7.1 (*80*) and counted using RSEM v.1.28. Differential gene expression analysis was performed using the DESEQ2 R package v1.22.2 (*81*) in R 3.5.2. GSEA analysis was performed using the fgsea R package v1.8.8 in R 3.5.2. (*82*) was run on DESEQ2 normalized counts using standard parameters with 1000 permutations and the log2foldchange as ranking metric. Following gene sets were used for analysis : H collection MSigDB hallmark gene sets (*45*). For GSEA analysis of predicted Let-7 target genes, the *let-7-5p_miR-98-5p_top 100_score predicted_targets* were obtained from *TargetScan7.2*: (*83*). Data is made available in the GEO repository (GEO:#####).

qPCR

Total RNA was isolated using RNAzol (Sigma-Aldrich). cDNA synthesis was performed using the Taqman RT reagent kit (Life Technologies) according to manufacturer's instructions. qPCR analysis was done using probes from IDT technologies (*Myc* Mm.PT.39a.22214843.g and *Actb* Mm.PT.58.28494642, Lin28b Mm.PT.58.8558661) and master mix from Kapa Biosystems.

Western blot

Cells were lysed in lysis buffer (50mM Tris-HCl pH 7.8, 150 mM NaCl, 1 mM EDTA, 1% Nonidet P-40). Loading samples were prepared with Laemmli buffer (Bio-Rad) with β-mercaptoethanol (Scharlau Chemicals) and protease inhibitor (Roche). Proteins were separated by SDS–PAGE (12% Mini-Protean TGX gel, Bio-Rad) and transferred to a nitrocellulose

membrane (Trans-Blot Turbo™ Mini Nitrocellulose Transfer Packs, Bio-Rad). Membranes were blocked for 1h at room temperature in 5% BSA, 5% skimmed milk or 5% ECL blocking solution in TBS-0.05% Tween20; depending on the manufacturers instructions. Following primary antibodies were used: c-MYC (Y69) (Abcam #ab32072), human Lin28b (cell signaling technologies #4196), murine Lin28b (Abcam #ab71415), pGSK3B(Ser9) (cell signaling technologies #5558), pPDK1 (Ser241) (cell signaling technologies #3438), pS6 (cell signaling technologies #2211) and β-Actin (sigma aldrich #A1978). The membrane was then incubated with VeriBlot secondary antibody (Abcam) for one hour at room temperature. Antibodies were used at the recommended concentrations. The ECL Prime kit (GE Healthcare) was used to detect protein bands with a ChemiDoc XRS+ system (Bio-Rad). All reagents were used according to the manufacturers instructions.

Statistical analysis

All statistical analysis was performed using Graphpad Prism v7. Statistical significant was tested using a two-sided unpaired t-test, unless otherwise specified in the figure legend. Statistical analysis of RNAseq data was obtained through analysis in the cited R packages.

Figure legends

Figure 1. Establishing a positive correlation between CD5 expression and self-reactivity in BCR wildtype B-1 cells.

(A) Flow cytometric analysis of peritoneal cavity (PerC) B cells 16 weeks after transplantation of E14.5 FL or adult bone marrow (ABM) Lin–Sca1+cKit+ (LSK) HSPCs into lethally irradiated CD45.1^{+}CD45.2^{+} congenic recipients. Lineage panel for E14.5 FL LSK: Ter119$^{–}$ B220$^{–}$Gr1$^{–}$ CD3e$^{–}$ and ABM LSK: Ter119$^{–}$B220$^{–}$Gr1$^{–}$CD11b$^{–}$CD3e$^{–}$. Lineage panel for PerC B cells: Ter119$^{–}$Gr1$^{–}$CD3e$^{–}$**(B)** CD5^{neg}, CD5^{low}, CD5^{int} and CD5^{hi} gating strategy for WT adult peritoneal cavity B-1 cells (Lin$^{–}$CD19^{+}CD43^{+}CD23$^{–}$). **(C)** Histogram overlay showing postsort analysis of the populations defined in B. **(D)** Relative distribution of IgHM CDR3 sequences as determined by high-throughput VDJseq of the indicated B-1 populations. **(E)** Gini index of IgHM CDR3 sequence reads in sorted CD5^{neg}, CD5^{low}, CD5^{int} and CD5^{hi} populations (left to right). **(F)** Stacked bargraph indicates the combined frequency of IGHV-11 (white) and IGHV-12 (grey) containing IgHM CDR3 sequence reads. **(G)** Frequency of PtC liposome reactive cells in the indicated B-1 populations as assessed by FACS analysis. (n=9 biological replicates, from 3 independent experiments) **(H)** Frequency of CDR3 containing one or more N-nucleotide additions at the N1 and N2 VDJ junctions combined. VDJseq data (B-F,H) is representative of two biological and technical replicates. Significance was tested using an unpaired t-test in panel in G. Ns=not significant, *=P ≤ 0.05, ***=P ≤ 0.001, ****=P≤ 0.0001.

Figure 2. Lin28b promotes the positive selection of CD5^{+} immature B cells in neonatal mice

(A) Representative histogram overlay of CD5 surface expression on 2-day-old neonatal bone marrow (NBM) and 4-month-old ABM small pre-B cells (Lin$^{–}$CD19^{+}CD93^{+}IgM$^{–}$CD43$^{–}$ CD24^{high}FSC^{low}) and immature B cells (ImmB) (Lin$^{–}$CD19^{+}CD93^{+}IgM^{+}CD24^{high}). Lineage panel for BM B cells (Ter119$^{–}$Gr1$^{–}$CD11b$^{–}$CD3e$^{–}$). Lower panel shows the CD5 fluorescence intensity interquartile ranges (IQR) of the same populations. Q1= 25th percentile, Q3=75th percentile, M= median. **(B)** CD5 levels on PtC liposome reactive and total ImmB cells from 2-day-old WT NBM. **(C)** Histogram overlay of CD5 levels on 2-day-old NBM ABM of the indicated genotypes. Lower panel shows the CD5 IQR. **(D)** Representative FACS plots showing the frequency of Lineage$^{–}$(CD3e$^{–}$Gr1$^{–}$Ter119$^{–}$) CD19^{+}CD5^{+} B-1 cells in the PerC from 10 day old neonatal mice of the indicated genotypes. **(E)** Quantification of data shown in panel D (n=4-7 biological replicates from 3 independent experiments). **(F)** Representative histogram overlays

of CD5 surface expression on 2-day-old, 5-day-old, 10-day-old and 19-day-old WT BM and 4-month-old WT ABM. **(G)** Quantification of relative cell size of ImmB from mice of the indicated genotypes and ages. Data are shown as a value relative to the size of a representative Lin28b$^{+/+}$ 2-day-old NBM (n=3-7 biological replicates from 3 independent experiments). Significance was tested using an unpaired t-test. ns=not significant, **=P ≤ 0.01, ***=P ≤ 0.001, ****=P≤ 0.0001.

Figure 3. Ectopic expression of Lin28b is sufficient to support enhanced B cell positive selection in the adult.

(A) Representative histogram overlay of CD5 surface expression on DOX fed tet-Lin28b and WT ABM small pre-B cells and ImmB cells. Lower panel shows the CD5 IQR of the populations in the upper panel. **(B)** Quantification of relative forward scatter (FSC-A) of pro-B, small pre-B and ImmB from tet-Lin28b ABM as measured by FACS. The ratio of tet-Lin28b/WT cells from each experiment were calculated and plotted (n=5 biological replicates from 3 independent experiments). Statistics were performed using a parametric t-test of the ratios against the value 1 (no change) **(C)** Sort strategy for isolation of the 20% highest and lowest CD5 expressing ABM ImmB from DOX fed tet-Lin28b mice. Sorted cells were transplanted intraperitoneally into untreated RAG1KO recipient mice on a normal diet. **(D)** Frequency of PerC CD5^{+} B-1 cells 3 weeks after transplantation (n=3 biological replicates from 2 independent experiments). **(E)** Representative histogram overlay of CD5 surface expression on PerC B-1 cells 3 weeks after transplantation. **(F)** Representative FACS analysis of PtC liposome reactivity of PerC B-1 cells 3 weeks after transplantation. Significance was tested using an unpaired t-test, ns=not significant, ***=P ≤ 0.001, ****=P≤ 0.0001. Where indicated, mice were fed a DOX diet for at least 10 days.

Figure 4. Lin28b alters the efficiency of overall B cell selection.

(A) Schematic showing the cellular barcoding setup of pro-B cells. 1x10^{5} tet-Lin28b pro-B cells (Lin^{-}CD19^{+}IgM^{-}CD93^{+}cKit^{+}CD43^{+}CD24^{lo}CD25^{-}) were sorted from untreated mice and transduced with barcode-GFP-LV in culture. Transduced cells were divided into two equal parts that were individually adoptively transferred into DOX fed and untreated Rag1KO recipients respectively. Barcode representation of mature splenic B cell progeny CD19^{+}CD93^{-}GFP^{+}) was assessed 2 weeks following adoptive transfer. **(B)** Stacked bars show representative read frequencies of individual barcodes retrieved. Number on top of bars indicate the number of unique barcodes detected in both PCR technical replicates (For more details see Figure S3). **(C)**

Enumeration of the barcodes retrieved from splenic mature B cells (n=5 biological replicates from 2 independent experiments). **(D)** Representative dot plots showing splenic mature B cells 2 weeks post transfer. **(E)** Histogram overlay show representative CD5 expression of splenic mature B-1 ($GFP^+CD19^+CD93^-CD43^+CD23^-$) and follicular B-2 subsets ($GFP^+CD19^+CD93^-CD43^-CD23^+$) 2 weeks post transfer. **(F-H)** Kinetics of Edu label progression during B cell development following administration of a single pulse of Edu into tet-Lin28b and WT mice fed on a DOX diet for at least 10 days prior to labelling. Edu labelling at the indicated timepoints was assessed by FACS and plotted for the indicated populations (n=3-4 biological replicates in each group, from 2-3 independent experiments). Significance was tested using a paired t-test **(C)** or unpaired t-test **(F-H)**. ns= not significant, *=$P \leq 0.05$. Error bars show the standard deviation (SD) of the mean.

Figure 5. Lin28b promotes B cell positive selection through activation the cMyc transcriptional program

(A) Volcano plot showing differentially expressed genes in immature B cells from WT ABM or tet-Lin28b ABM fed doxycycline food for 2 weeks. **(B)** Normalized DESeq counts for the depicted genes (from (A)). **(C)** (left) GSEA analysis testing for significantly enriched gene sets among the hallmark collection and (right) Top enriched hallmark gene sets based on the data shown in A. **(D)** Leading edge plots showing hallmark MYC Targets V1, hallmark Interferon Gamma and Targetscan Top 100 Let-7 targets based on data shown in A. **(E)** Normalized DESeq counts and qPCR analysis of Myc transcript levels in immature B cells from WT ABM or tet-Lin28b ABM fed doxycycline food for 2 weeks (n=3 biological replicates) **(F)** Western blot analysis of cMYC and Lin28b transgene protein levels in sorted ABM ImmB cells. **(G)** Histogram overlays showing c-Myc protein expression as measured by intracellular FACS in 3-day-old NBM and ABM ImmB cells from the indicated genotypes. **(H)** Western blot analysis showing c-Myc protein expression in 3-day-old NBM and spleen cells from the indicated genotypes. **(I)** (Left) Top enriched hallmark gene sets and (right) leading edge plot showing hallmark MYC Targets V1 based on differentially expressed genes in immature B cells from WT and $Lin28b^{-/-}$ 3-day old NBM

Figure 6. Ectopic Lin28b functionally replaces CD19 in B cell development and maintenance

(A) Representative FACS plots depicting splenic B cells in DOX fed adult mice of the indicated genotypes. **(B)** (left) Quantification of data shown in A. (right) Absolute B cell numbers in

spleen of mice with the indicated genotypes. **(C)** CD5 levels on ABM ImmB cells from DOX fed mice of the indicated genotypes (n=5-7, from 3 independent experiments). **(D)** Representative FACS plots showing kappa and lambda light chain usage in ABM ImmB cells from DOX fed mice of the indicated genotypes. **(E)** Quantification of data shown in D (n=4-9, from 3 independent experiments). **(F)** Representative western blot depicting pPDK1, pGSK3b, c-Myc, human Lin28b (tg-Lin28b), pS6 and b-Actin levels in lineage depleted ($CD3^{-}Gr1^{-}$ $CD11b^{-}Ter119^{-}$) spleen cells. Western blot is representative of at least 3 representative biological and technical replicates. **(G)** Representative histogram depicting pS6 levels in immature B cells from WT ABM and tet-Lin28b ABM on doxycycline food (representative for 3 independent experiments). **(H)** Schematic depicting the proposed CD19/c-MYC/Lin28b positive feedback loop in neonatal and adult mice. Where indicated, mice were kept on a DOX diet for 3 weeks.

Figure 7. tet-Lin28b induced positive selection in the adult produces fully functional $CD5^{+}$ B-1 cells

(A) Schematic showing the DOX-STOP experimental set-up. 10.000 LSK HSPCs were sorted from the indicated donors and transplanted into sublethally irradiated Rag1KO recipients. Recipients were kept on a DOX diet for 4 weeks, allowing for transient B-1 cell output by tet-Lin28b HSPCs, followed by normal diet for 12 weeks (Figure S6). **(B)** Gating strategy for FACS sorting of PerC $CD5^{+}$ B-1 cells isolated from untransplanted adult (16-week-old) WT mice (nB-1) or the indicated reconstituted recipients 16-weeks after transplantation. **(C)** Frequency of PerC $CD5^{+}$ B-1 cells 16-weeks after transplantation (n=7-14, from 3 independent experiments). **(D)** $2x10^{4}$ sorted $CD5^{+}$ B-1cells from the indicated mice were competitively transferred by intraperitoneal injection along with congenic nB-1 competitors at a 1:2 ratio. Bar graph shows donor:competitor recovery ratio 12 weeks post transfer (n=4-6 biological replicates, from 2 independent experiments). **(E)** Histogram overlay showing CD5 expression levels of transferred nB-1, FLB-1, ABMB-1, L28B-1 cells and their congenic competitors. **(F)** Frequency of CDR3 containing one or more N-nucleotide additions at the N1and N2 VDJ junctions combined. VDJseq data is representative of 3-7 biological replicates, from 3 independent experiments. **(G)** IL-10 production by the indicated populations as determined by ELISA following 36hr of 10ug/ml LPS stimulation (n=2-3 biological replicates, from 2 independent experiments). **(H)** Spontaneous IgM production by splenic $CD5^{+}$ B-1 ($CD19^{+}CD1d^{-}CD23^{-}CD43^{+}$) and B-2 populations from the indicated mice as determined by ELISPOT (n=3-5 biological replicates, from 2 independent experiments). Significance was

tested using an unpaired test. ns= not significant, *= $P \leq 0.05$, **= $P \leq 0.01$, ****= $P \leq 0.0001$. Bars show the mean, error bars show the standard deviation (SD) of the mean. **(I)** Graphical summary. Our data put forward a unified model for the superior B-1 cell output early in life. In this model, Lin28b dependent immature B cell positive selection early in life endows B-1 cells with their hallmark characteristics including a stable CD5 expression profile and long-term fitness. Ectopic Lin28b in adult life can efficiently induce B-1 cell positive selection on the backdrop of a highly diverse adult type BCR junctional diversity. Adult derived B-1 cells that develop independently of Lin28b are functionally comparable in terms of IL-10 and spontaneous IgM secretion but display reduced CD5 expression and impaired long-term fitness. We propose that Lin28b mediated enhancement of B cell tonic signaling licenses self-reactive B-1 cell output during the neonatal period when the risk for harmful autoreactivity is constrained by limited junctional diversity, thereby contributing to an important layer of polyreactive natural antibody mediated immunity.

Acknowledgments: We thank Drs Jeremy A Daniel and Timothy P Bender for their critical input.

Funding: Grants to J.Y. from the European Research Council (715313), the Swedish Research Council, the Knut and Alice Wallenberg Foundation, and the Wenner-gren Foundations and grants to J.Y., and E.J.G from the Swedish Cancer Society.

Author Contributions: J.Y, S.Vanhee and E.J.G. designed the study. S.Vanhee, E.J.G., H.Å., T.A.K., S.D., G.M., K.O., A.D. and S.Vergani., performed the experiments. S.Vanhee performed the computational analyses together with S.L., S.S. and J.U.. C.J., G.B, C.B. and M.S. provided critical expertise and reagents. J.Y., conceived the study and wrote the paper together with S.Vanhee.

Competing interests: The authors declare no competing interests.

Data and aterials availability: The data for this study have been deposited in the database XXX.

References

1. N. Vrisekoop, J. P. Monteiro, J. N. Mandl, R. N. Germain, Revisiting thymic positive selection and the mature T cell repertoire for antigen. *Immunity* **41**, 181-190 (2014).

2. J. Lang *et al.*, B cells are exquisitely sensitive to central tolerance and receptor editing induced by ultralow affinity, membrane-bound antigen. *The Journal of experimental medicine* **184**, 1685-1697 (1996).

3. D. Nemazee, Receptor editing in lymphocyte development and central tolerance. *Nature reviews. Immunology* **6**, 728-740 (2006).

4. S. Shivtiel, N. Leider, O. Sadeh, Z. Kraiem, D. Melamed, Impaired Light Chain Allelic Exclusion and Lack of Positive Selection in Immature B Cells Expressing Incompetent Receptor Deficient of CD19. *The Journal of Immunology* **168**, 5596-5604 (2002).

5. E. Diamant, Z. Keren, D. Melamed, CD19 regulates positive selection and maturation in B lymphopoiesis: lack of CD19 imposes developmental arrest of immature B cells and consequential stimulation of receptor editing. *Blood* **105**, 3247-3254 (2005).

6. L. Verkoczy *et al.*, Basal B cell receptor-directed phosphatidylinositol 3-kinase signaling turns off RAGs and promotes B cell-positive selection. *Journal of immunology* **178**, 6332-6341 (2007).

7. L. E. Tze *et al.*, Basal immunoglobulin signaling actively maintains developmental stage in immature B cells. *PLoS Biol* **3**, e82 (2005).

8. N. Baumgarth, B-1 Cell Heterogeneity and the Regulation of Natural and Antigen-Induced IgM Production. *Frontiers in immunology* **7**, 324 (2016).

9. K. Hayakawa *et al.*, Positive selection of natural autoreactive B cells. *Science* **285**, 113-116 (1999).

10. R. Wasserman *et al.*, A Novel Mechanism for B Cell Repertoire Maturation Based on Response by B Cell Precursors to Pre–B Receptor Assembly. *Journal of Experimental Medicine*, (1998).

11. L. W. Arnold, C. A. Pennell, S. K. McCray, S. H. Clarke, Development of B-1 cells: segregation of phosphatidyl choline-specific B cells to the B-1 population occurs after immunoglobulin gene expression. *The Journal of experimental medicine* **179**, 1585-1595 (1994).

12. H. Ferry, T. L. Crockford, J. C. Leung, R. J. Cornall, Signals from a self-antigen induce positive selection in early B cell ontogeny but are tolerogenic in adults. *Journal of immunology* **176**, 7402-7411 (2006).

13. N. Shyh-Chang, G. Q. Daley, Lin28: primal regulator of growth and metabolism in stem cells. *Cell stem cell* **12**, 395-406 (2013).

14. J. Yuan, C. K. Nguyen, X. Liu, C. Kanellopoulou, S. A. Muljo, Lin28b reprograms adult bone marrow hematopoietic progenitors to mediate fetal-like lymphopoiesis. *Science* **335**, 1195-1200 (2012).

15. T. A. Kristiansen *et al.*, Cellular Barcoding Links B-1a B Cell Potential to a Fetal Hematopoietic Stem Cell State at the Single-Cell Level. *Immunity* **45**, 346-357 (2016).

16. R. G. Rowe *et al.*, Developmental regulation of myeloerythroid progenitor function by the Lin28b-let-7-Hmga2 axis. *The Journal of experimental medicine* **213**, 1497-1512 (2016).

17. M. R. Copley *et al.*, The Lin28b-let-7-Hmga2 axis determines the higher self-renewal potential of fetal haematopoietic stem cells. *Nature cell biology* **15**, 916-925 (2013).

18. J. Wang *et al.*, Fetal and adult progenitors give rise to unique populations of CD8+ T cells. *Blood* **128**, 3073-3082 (2016).

19. M. C. Stolla *et al.*, Lin28b regulates age-dependent differences in murine platelet function. *Blood Adv* **3**, 72-82 (2019).

20. Y. Zhou *et al.*, Lin28b promotes fetal B lymphopoiesis through the transcription factor Arid3a. *The Journal of experimental medicine* **212**, 569-580 (2015).

21. R. Berland, H. H. Wortis, Origins and functions of B-1 cells with notes on the role of CD5. *Annual review of immunology* **20**, 253-300 (2002).

22. P. Casali, A. L. Notkins, CD5+ B lymphocytes, polyreactive antibodies and the human B-cell repertoire. *Immunol Today* **10**, 364-368 (1989).

23. H. S. Azzam *et al.*, CD5 expression is developmentally regulated by T cell receptor (TCR) signals and TCR avidity. *The Journal of experimental medicine* **188**, 2301-2311 (1998).

24. J. N. Mandl, J. P. Monteiro, N. Vrisekoop, R. N. Germain, T cell-positive selection uses self-ligand binding strength to optimize repertoire recognition of foreign antigens. *Immunity* **38**, 263-274 (2013).

25. K. L. Hippen, L. E. Tze, T. W. Behrens, CD5 maintains tolerance in anergic B cells. *The Journal of experimental medicine* **191**, 883-890 (2000).

26. L. Wen *et al.*, Evidence of marginal-zone B cell-positive selection in spleen. *Immunity* **23**, 297-308 (2005).

27. E. Y. Chung *et al.*, CD19 is a major B cell receptor-independent activator of MYC-driven B-lymphomagenesis. *The Journal of clinical investigation* **122**, 2257-2266 (2012).

28. J. C. Poe, V. Minard-Colin, E. I. Kountikov, K. M. Haas, T. F. Tedder, A c-Myc and surface CD19 signaling amplification loop promotes B cell lymphoma development and progression in mice. *Journal of immunology* **189**, 2318-2325 (2012).

29. D. Benhamou *et al.*, A c-Myc/miR17-92/Pten Axis Controls PI3K-Mediated Positive and Negative Selection in B Cell Development and Reconstitutes CD19 Deficiency. *Cell Rep* **16**, 419-431 (2016).

30. S. Duber *et al.*, Induction of B-cell development in adult mice reveals the ability of bone marrow to produce B-1a cells. *Blood* **114**, 4960-4967 (2009).

31. N. E. Holodick, T. Vizconde, T. L. Rothstein, B-1a cell diversity: nontemplated addition in B-1a cell Ig is determined by progenitor population and developmental location. *Journal of immunology* **192**, 2432-2441 (2014).

32. C. M. Sawai *et al.*, Hematopoietic Stem Cells Are the Major Source of Multilineage Hematopoiesis in Adult Animals. *Immunity* **45**, 597-609 (2016).

33. A. B. Kantor, A. M. Stall, S. Adams, L. A. Herzenberg, L. A. Herzenberg, Differential development of progenitor activity for three B-cell lineages. *Proceedings of the National Academy of Sciences of the United States of America* **89**, 3320-3324 (1992).

34. M. Bogue, S. Gilfillan, C. Benoist, D. Mathis, Regulation of N-region diversity in antigen receptors through thymocyte differentiation and thymus ontogeny. *Proceedings of the National Academy of Sciences of the United States of America* **89**, 11011-11015 (1992).

35. H. Wardemann *et al.*, Predominant autoantibody production by early human B cell precursors. *Science* **301**, 1374-1377 (2003).

36. G. K. Pedersen *et al.*, B-1a transitional cells are phenotypically distinct and are lacking in mice deficient in IkappaBNS. *Proceedings of the National Academy of Sciences of the United States of America* **111**, E4119-4126 (2014).

37. G. Shinoda *et al.*, Fetal deficiency of lin28 programs life-long aberrations in growth and glucose metabolism. *Stem cells* **31**, 1563-1573 (2013).

38. H. Zhu *et al.*, The Lin28/let-7 axis regulates glucose metabolism. *Cell* **147**, 81-94 (2011).

39. S. H. Naik, T. N. Schumacher, L. Perie, Cellular barcoding: a technical appraisal. *Experimental hematology* **42**, 598-608 (2014).

40. R. Lu, N. F. Neff, S. R. Quake, I. L. Weissman, Tracking single hematopoietic stem cells in vivo using high-throughput sequencing in conjunction with viral genetic barcoding. *Nature biotechnology* **29**, 928-933 (2011).

41. R. R. Hardy, K. Hayakawa, M. Shimizu, K. Yamasaki, T. Kishimoto, Rheumatoid factor secretion from human Leu-1+ B cells. *Science* **236**, 81-83 (1987).

42. J. H. Antin, S. G. Emerson, P. Martin, N. Gadol, K. A. Ault, Leu-1+ (CD5+) B cells. A major lymphoid subpopulation in human fetal spleen: phenotypic and functional studies. *Journal of immunology* **136**, 505-510 (1986).

43. M. Bofill *et al.*, Human B cell development. II. Subpopulations in the human fetus. *Journal of immunology* **134**, 1531-1538 (1985).

44. J. Zikherman, R. Parameswaran, A. Weiss, Endogenous antigen tunes the responsiveness of naive B cells but not T cells. *Nature* **489**, 160-164 (2012).

45. A. Liberzon *et al.*, The Molecular Signatures Database (MSigDB) hallmark gene set collection. *Cell Syst* **1**, 417-425 (2015).

46. V. B. Sampson *et al.*, MicroRNA let-7a down-regulates MYC and reverts MYC-induced growth in Burkitt lymphoma cells. *Cancer research* **67**, 9762-9770 (2007).

47. S. Manier *et al.*, The LIN28B/let-7 axis is a novel therapeutic pathway in multiple myeloma. *Leukemia* **31**, 853-860 (2017).

48. T. C. Chang *et al.*, Lin-28B transactivation is necessary for Myc-mediated let-7 repression and proliferation. *Proceedings of the National Academy of Sciences of the United States of America* **106**, 3384-3389 (2009).

49. X. Jiang *et al.*, Blockade of miR-150 maturation by MLL-fusion/MYC/LIN-28 is required for MLL-associated leukemia. *Cancer cell* **22**, 524-535 (2012).

50. N. Shyh-Chang *et al.*, Lin28 enhances tissue repair by reprogramming cellular metabolism. *Cell* **155**, 778-792 (2013).

51. L. Srinivasan *et al.*, PI3 kinase signals BCR-dependent mature B cell survival. *Cell* **139**, 573-586 (2009).

52. G. V. Baracho *et al.*, PDK1 regulates B cell differentiation and homeostasis. *Proceedings of the National Academy of Sciences of the United States of America* **111**, 9573-9578 (2014).

53. A. N. Anzelon, H. Wu, R. C. Rickert, Pten inactivation alters peripheral B lymphocyte fate and reconstitutes CD19 function. *Nature immunology* **4**, 287-294 (2003).

54. P. Engel *et al.*, Abnormal B lymphocyte Development, Activation, and Differentiation in Mice that LAck or Overexpress the CD19 Signal Transduction Molecule. *Immunity*, (1995).

55. R. C. Rickert, K. Rajewsky, J. Roes, Impairment of T-cell-dependent B-cell responses and B-1 cell development in CD19-deficient mice. *Nature* **376**, 352-355 (1995).

56. D. C. Otero, A. N. Anzelon, R. C. Rickert, CD19 Function in Early and Late B Cell Development: I. Maintenance of Follicular and Marginal Zone B Cells Requires CD19-Dependent Survival Signals. *The Journal of Immunology* **170**, 73-83 (2003).

57. Z. Hao, K. Rajewsky, Homeostasis of peripheral B cells in the absence of B cell influx from the bone marrow. *The Journal of experimental medicine* **194**, 1151-1164 (2001).

58. S. Sato, N. Ono, D. A. Steeber, D. S. Pisetsky, T. F. Tedder, CD19 regulates B lymphocyte signaling thresholds critical for the development of B-1 lineage cells and autoimmunity. *Journal of immunology* **157**, 4371-4378 (1996).

59. M. Inaoki, S. Sato, B. C. Weintraub, C. C. Goodnow, T. F. Tedder, CD19-regulated signaling thresholds control peripheral tolerance and autoantibody production in B lymphocytes. *The Journal of experimental medicine* **186**, 1923-1931 (1997).

60. A. Gonzalez-Martin *et al.*, The microRNA miR-148a functions as a critical regulator of B cell tolerance and autoimmunity. *Nature immunology* **17**, 433-440 (2016).

61. M. Coffre *et al.*, miRNAs Are Essential for the Regulation of the PI3K/AKT/FOXO Pathway and Receptor Editing during B Cell Maturation. *Cell Rep* **17**, 2271-2285 (2016).

62. S. Sander *et al.*, Synergy between PI3K signaling and MYC in Burkitt lymphomagenesis. *Cancer cell* **22**, 167-179 (2012).

63. E. Koscianska *et al.*, Prediction and preliminary validation of oncogene regulation by miRNAs. *BMC Mol Biol* **8**, 79 (2007).

64. S. Wang *et al.*, Enhancement of LIN28B-induced hematopoietic reprogramming by IGF2BP3. *Genes & development*, (2019).

65. K. Hayakawa *et al.*, Crucial Role of Increased Arid3a at the Pre-B and Immature B Cell Stages for B1a Cell Generation. *Frontiers in immunology* **10**, (2019).

66. E. M. Staley, A. Z. Feldman, R. G. Koenig, B. Hill, CD5 positive B-ALL, a uniquely aggressive subcategory of B-ALL? A case report and brief review of the literature. *Pediatr Blood Cancer* **66**, e27484 (2019).

67. L. Chen, Y. Sun, J. Wang, H. Jiang, A. G. Muntean, Differential regulation of the c-Myc/Lin28 axis discriminates subclasses of rearranged MLL leukemia. *Oncotarget* **7**, 25208-25223 (2016).

68. E. Montecino-Rodriguez, K. Dorshkind, B-1 B cell development in the fetus and adult. *Immunity* **36**, 13-21 (2012).

69. A. B. Kantor, L. A. Herzenberg, Origin of murine B cell lineages. *Annual review of immunology* **11**, 501-538 (1993).

70. K. Hayakawa, R. R. Hardy, L. A. Herzenberg, L. A. Herzenberg, Progenitors for Ly-1 B cells are distinct from progenitors for other B cells. *The Journal of experimental medicine* **161**, 1554-1568 (1985).

71. S. Casola *et al.*, B cell receptor signal strength determines B cell fate. *Nature immunology* **5**, 317-327 (2004).

72. K. Rajewsky, The Herzenberg lecture: how to make a B-1 cell? *Ann N Y Acad Sci* **1362**, 6-7 (2015).

73. G. Haughton, L. W. Arnold, A. C. Whitmore, S. H. Clarke, B-1 cells are made, not born. *Immunol Today* **14**, 84-87; discussion 87-91 (1993).

74. R. Graf *et al.*, BCR-dependent lineage plasticity in mature B cells. *Science* **363**, 748-753 (2019).

75. J. J. Bunker *et al.*, Natural polyreactive IgA antibodies coat the intestinal microbiota. *Science* **358**, (2017).

76. H. Mouquet, M. C. Nussenzweig, Polyreactive antibodies in adaptive immune responses to viruses. *Cellular and molecular life sciences : CMLS* **69**, 1435-1445 (2012).

77. C. Lo Celso, D. Scadden, Isolation and transplantation of hematopoietic stem cells (HSCs). *Journal of visualized experiments : JoVE*, 157 (2007).

78. D. Su *et al.*, PTIP chromatin regulator controls development and activation of B cell subsets to license humoral immunity in mice. *Proceedings of the National Academy of Sciences of the United States of America* **114**, E9328-E9337 (2017).

79. Z. Gu, L. Gu, R. Eils, M. Schlesner, B. Brors, circlize Implements and enhances circular visualization in R. *Bioinformatics* **30**, 2811-2812 (2014).

80. A. Dobin *et al.*, STAR: ultrafast universal RNA-seq aligner. *Bioinformatics* **29**, 15-21 (2013).

81. M. I. Love, W. Huber, S. Anders, Moderated estimation of fold change and dispersion for RNA-seq data with DESeq2. *Genome biology* **15**, 550 (2014).

82. A. A. Sergushichev, An algorithm for fast preranked gene set enrichment analysis using cumulative statistic calculation. *bioRxiv*, (2016).

83. V. Agarwal, G. W. Bell, J. W. Nam, D. P. Bartel, Predicting effective microRNA target sites in mammalian mRNAs. *eLife* **4**, (2015).

Figure1

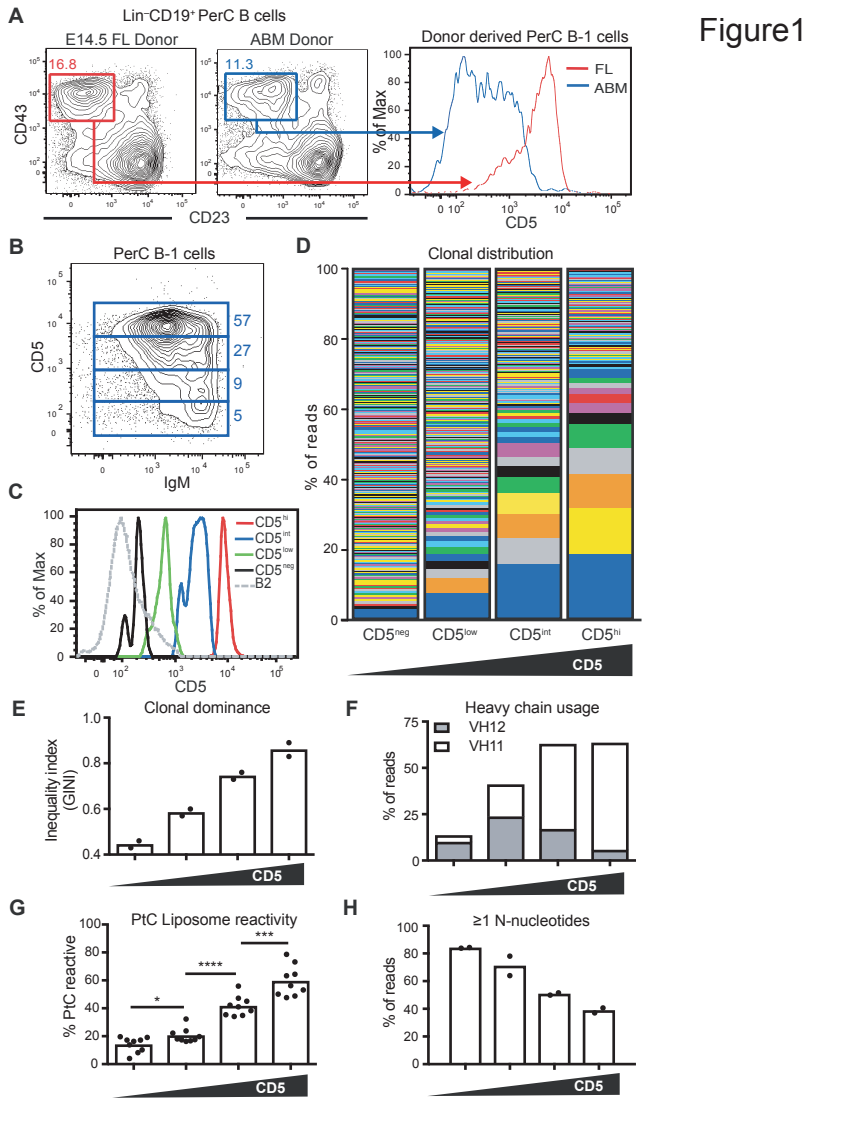
A
Lin-CD19+ PerC B cells
E14.5 FL Donor
ABM Donor
16.8
11.3
CD43
CD23
Donor derived PerC B-1 cells
% of Max
FL
ABM
CD5
B
PerC B-1 cells
CD5
IgM
57
27
9
5
C
% of Max
CD5hi
CD5int
CD5low
CD5neg
B2
CD5
D
Clonal distribution
% of reads
CD5neg
CD5low
CD5int
CD5hi
CD5
E
Clonal dominance
Inequality index (GINI)
CD5
F
Heavy chain usage
% of reads
VH12
VH11
CD5
G
PtC Liposome reactivity
% PtC reactive
*
****
***
CD5
H
≥1 N-nucleotides
% of reads
CD5

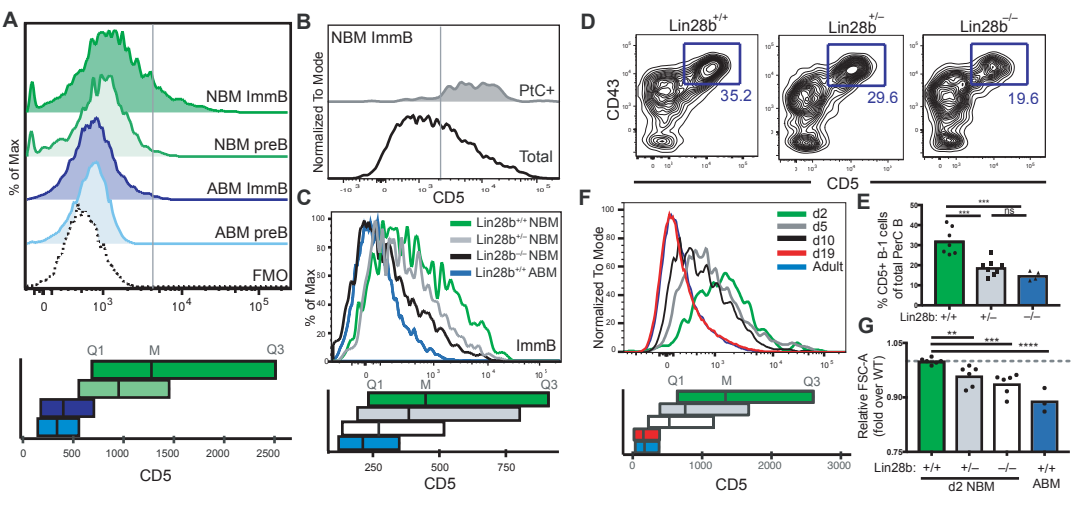
A
NBM ImmB
NBM preB
ABM ImmB
ABM preB
FMO
% of Max
Q1
M
Q3
CD5
B
NBM ImmB
PtC+
Total
Normalized To Mode
CD5
C
Lin28b+/+ NBM
Lin28b+/– NBM
Lin28b–/– NBM
Lin28b+/+ ABM
% of Max
ImmB
Q1
M
Q3
CD5
D
Lin28b+/+
Lin28b+/–
Lin28b–/–
CD43
35.2
29.6
19.6
CD5
F
d2
d5
d10
d19
Adult
Normalized To Mode
Q1
M
Q3
CD5
E
% CD5+ B-1 cells of total PerC B
ns
Lin28b: +/+
+/–
–/–
G
Relative FSC-A (fold over WT)
Lin28b: +/+
+/–
–/–
+/+
d2 NBM
ABM

Figure2

Figure3

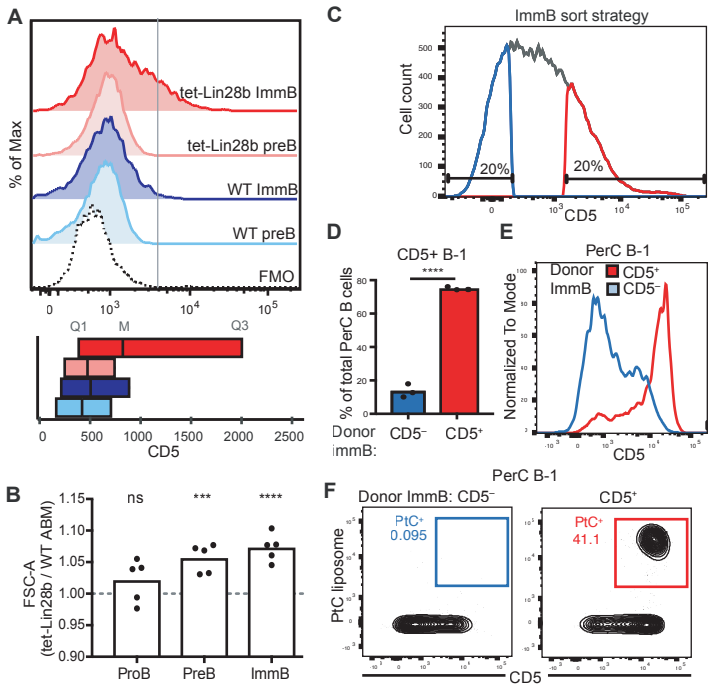
A
% of Max
tet-Lin28b ImmB
tet-Lin28b preB
WT ImmB
WT preB
FMO
Q1
M
Q3
CD5
C
ImmB sort strategy
Cell count
20%
20%
CD5
D
CD5+ B-1
****
% of total PerC B cells
Donor ImmB:
CD5⁻
CD5⁺
E
PerC B-1
Donor ImmB
CD5⁺
CD5⁻
Normalized To Mode
CD5
B
ns
***
****
FSC-A (tet-Lin28b / WT ABM)
ProB
PreB
ImmB
F
PerC B-1
Donor ImmB: CD5⁻
CD5⁺
PtC liposome
PtC⁺ 0.095
PtC⁺ 41.1
CD5

Figure4

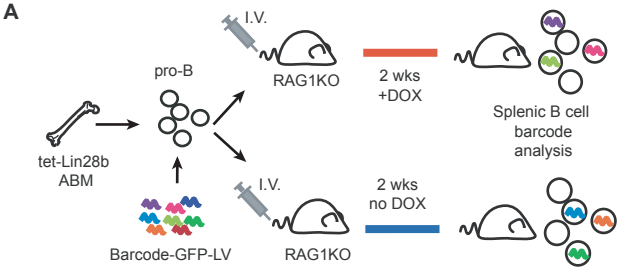
A
I.V.
RAG1KO
pro-B
2 wks
+DOX
Splenic B cell
barcode
analysis
tet-Lin28b
ABM
2 wks
no DOX
I.V.
Barcode-GFP-LV
RAG1KO

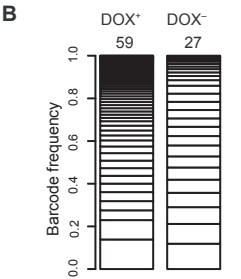
B
DOX+
DOX−
59
27
Barcode frequency
1.0
0.8
0.6
0.4
0.2
0.0

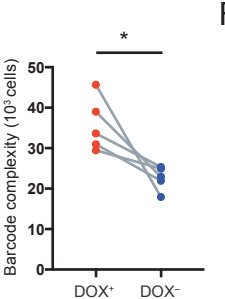
C
*
Barcode complexity (10³ cells)
50
40
30
20
10
0
DOX+
DOX−

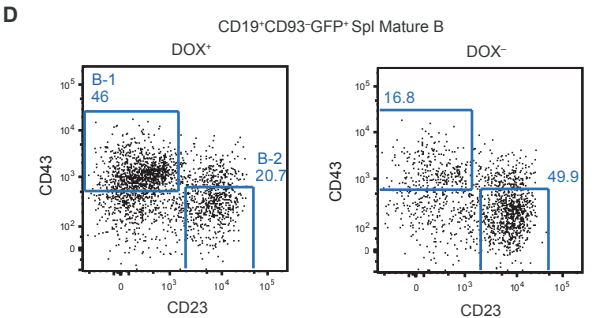
D
CD19+CD93-GFP+ Spl Mature B
DOX+
DOX−
B-1
46
B-2
20.7
16.8
49.9
CD43
CD23

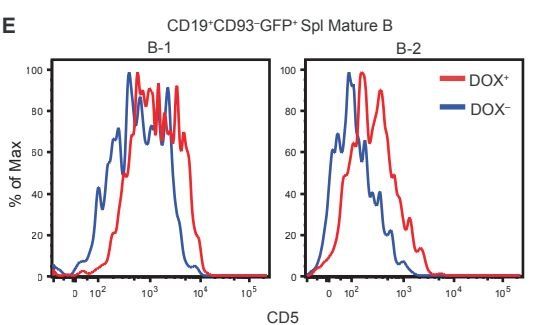
E
CD19+CD93-GFP+ Spl Mature B
B-1
B-2
DOX+
DOX−
% of Max
CD5

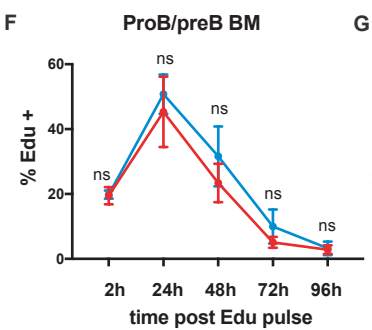
F
ProB/preB BM
% Edu +
ns
2h
24h
48h
72h
96h
time post Edu pulse

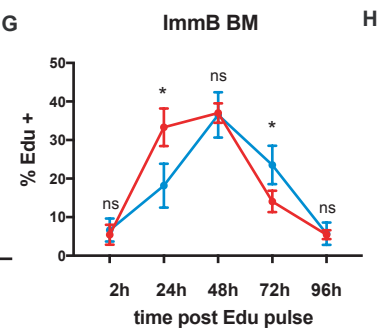
G
ImmB BM
% Edu +
*
ns
2h
24h
48h
72h
96h
time post Edu pulse

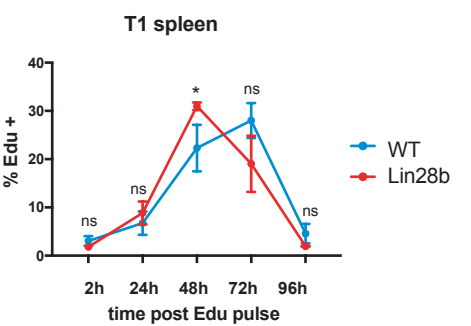
H
T1 spleen
% Edu +
*
ns
2h
24h
48h
72h
96h
time post Edu pulse
WT
Lin28b

Figure 5

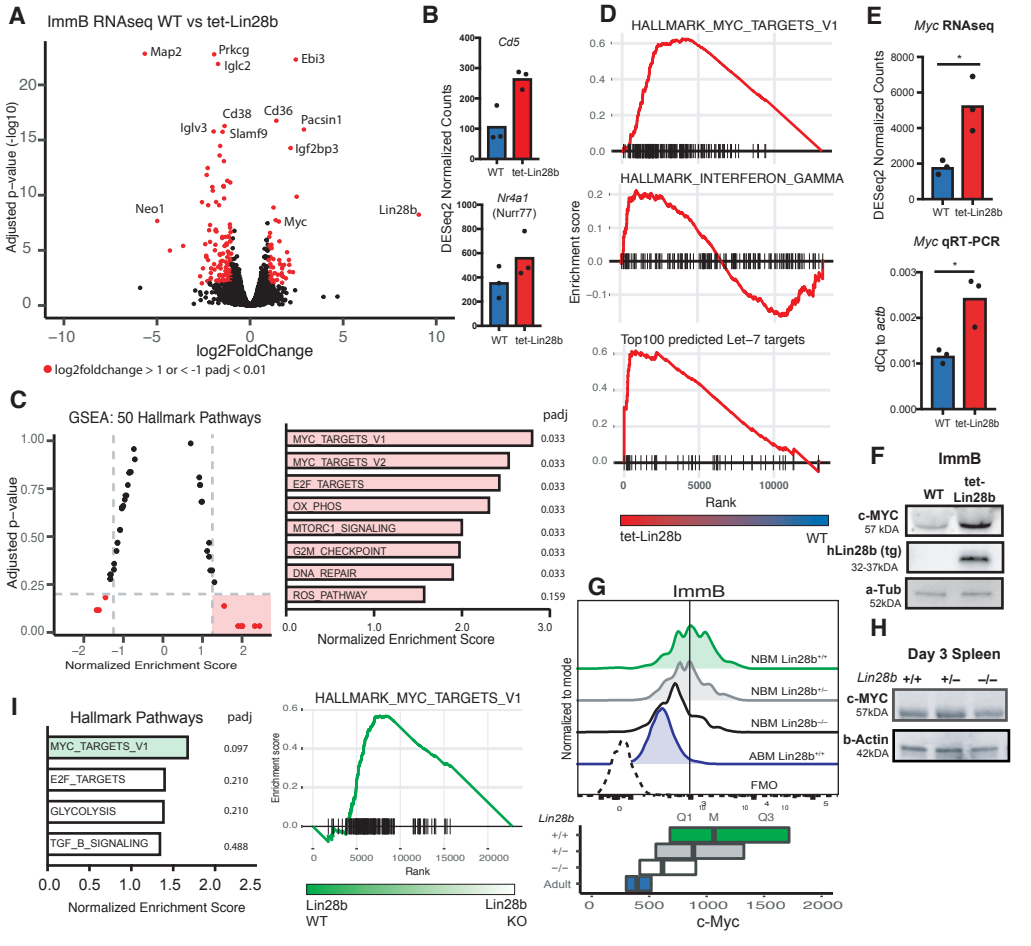
A
ImmB RNAseq WT vs tet-Lin28b
Map2
Prkcg
Iglc2
Ebi3
Cd38
Cd36
Pacsin1
Iglv3
Slamf9
Igf2bp3
Neo1
Myc
Lin28b
Adjusted p-value (-log10)
log2FoldChange
log2foldchange > 1 or < -1 padj < 0.01
B
Cd5
DESeq2 Normalized Counts
WT
tet-Lin28b
Nr4a1
(Nurr77)
D
HALLMARK_MYC_TARGETS_V1
HALLMARK_INTERFERON_GAMMA
Top100 predicted Let−7 targets
Enrichment score
Rank
tet-Lin28b
WT
E
Myc RNAseq
DESeq2 Normalized Counts
Myc qRT-PCR
dCq to actb
C
GSEA: 50 Hallmark Pathways
Adjusted p−value
Normalized Enrichment Score
padj
MYC_TARGETS_V1
MYC_TARGETS_V2
E2F_TARGETS
OX_PHOS
MTORC1_SIGNALING
G2M_CHECKPOINT
DNA_REPAIR
ROS_PATHWAY
F
ImmB
WT
tet-Lin28b
c-MYC
57 kDA
hLin28b (tg)
32-37kDA
a-Tub
52kDA
G
ImmB
Normalized to mode
NBM Lin28b+/+
NBM Lin28b+/−
NBM Lin28b−/−
ABM Lin28b+/+
FMO
Q1
M
Q3
Lin28b
+/+
+/−
−/−
Adult
c-Myc
H
Day 3 Spleen
Lin28b +/+ +/− −/−
c-MYC
57kDA
b-Actin
42kDA
I
Hallmark Pathways
padj
MYC_TARGETS_V1
E2F_TARGETS
GLYCOLYSIS
TGF_B_SIGNALING
Normalized Enrichment Score
HALLMARK_MYC_TARGETS_V1
Enrichment score
Rank
Lin28b
WT
Lin28b
KO

Figure6

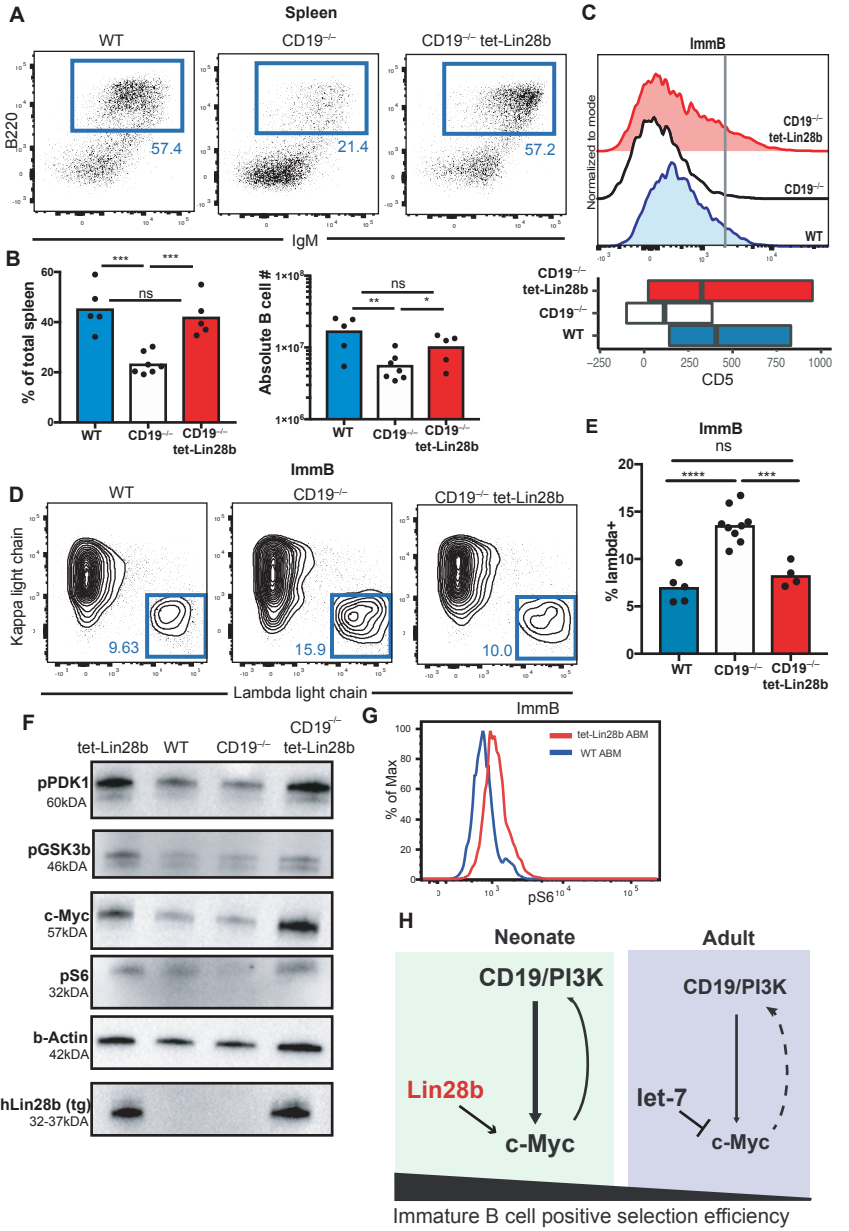

Immature B cell positive selection efficiency
CD5+ B-1 cell maturation

Figure7

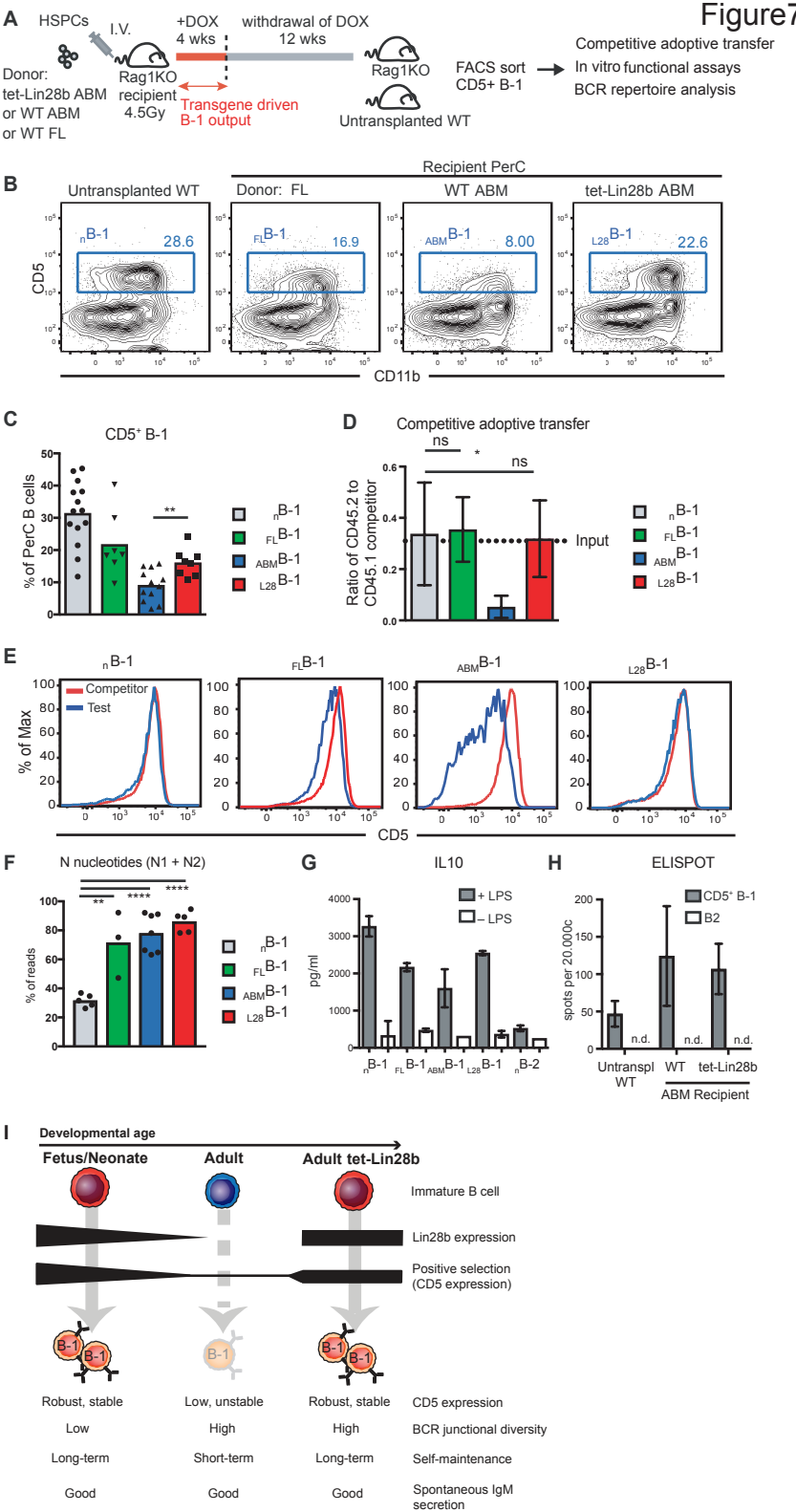
A
HSPCs
I.V.
+DOX
4 wks
withdrawal of DOX
12 wks
Donor:
tet-Lin28b ABM
or WT ABM
or WT FL
Rag1KO
recipient
4.5Gy
Transgene driven
B-1 output
Rag1KO
Untransplanted WT
FACS sort
CD5+ B-1
Competitive adoptive transfer
In vitro functional assays
BCR repertoire analysis
B
Recipient PerC
Untransplanted WT
Donor: FL
WT ABM
tet-Lin28b ABM
nB-1
28.6
FLB-1
16.9
ABMB-1
8.00
L28B-1
22.6
CD5
CD11b
C
CD5+ B-1
% of PerC B cells
D
Competitive adoptive transfer
ns
*
ns
Ratio of CD45.2 to CD45.1 competitor
Input
E
% of Max
Competitor
Test
CD5
F
N nucleotides (N1 + N2)
% of reads
G
IL10
+ LPS
– LPS
pg/ml
H
ELISPOT
CD5+ B-1
B2
spots per 20.000c
n.d.
Untranspl WT
WT
tet-Lin28b
ABM Recipient
I
Developmental age
Fetus/Neonate
Adult
Adult tet-Lin28b
Immature B cell
Lin28b expression
Positive selection
(CD5 expression)
Robust, stable
Low, unstable
Robust, stable
CD5 expression
Low
High
High
BCR junctional diversity
Long-term
Short-term
Long-term
Self-maintenance
Good
Good
Good
Spontaneous IgM
secretion

Supplemental figures

Figure S1

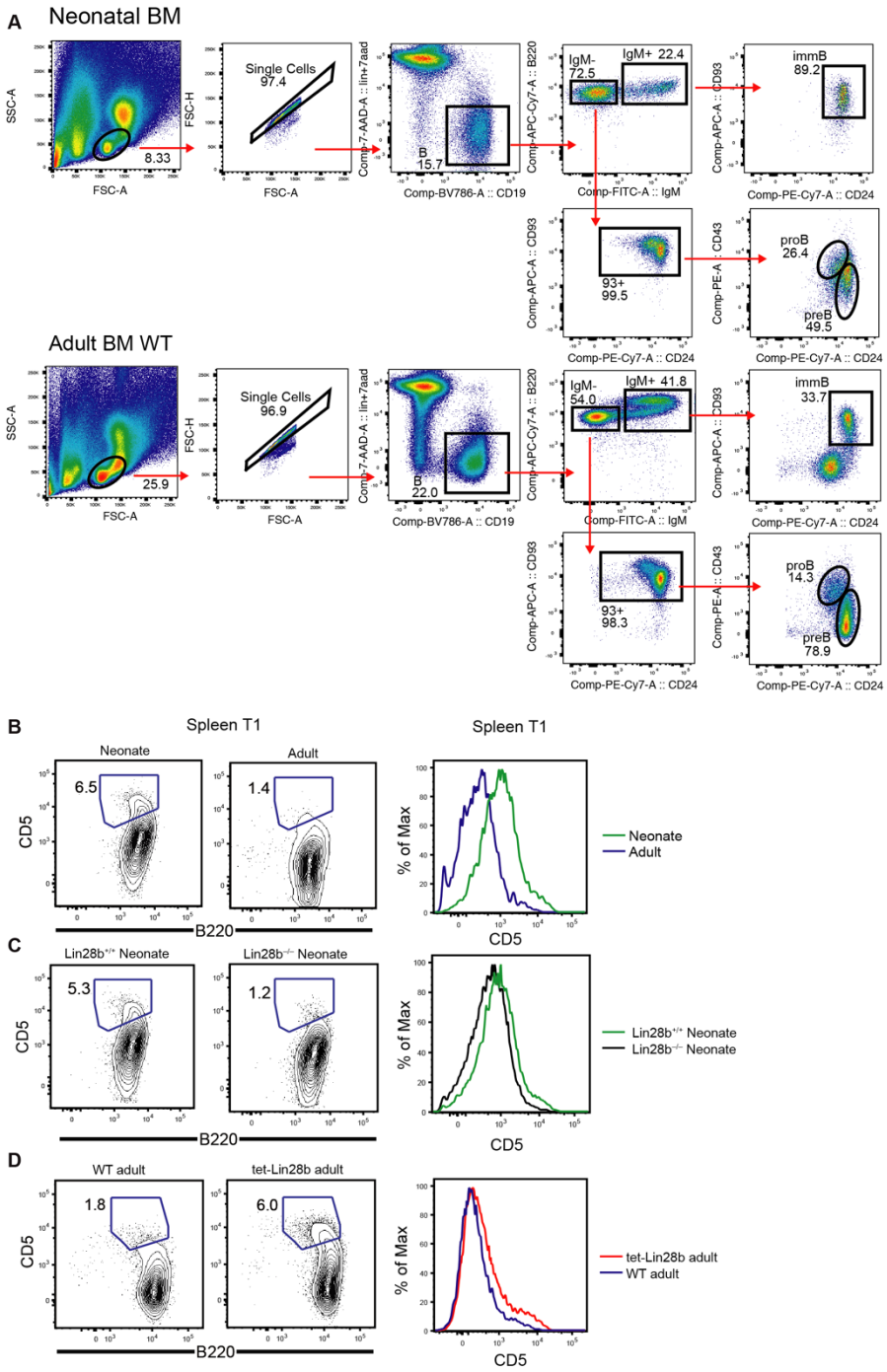

Figure S1; related to Figure 2 and Figure 3

(A) Gating strategy for proB, preB and immature B cells in bone marrow of neonatal and adult mice. **(B-C)** FACS analysis of CD5 levels on splenic T1 cells ($Lin^{-}CD19^{+}CD93^{+}CD23^{-}IgM^{+}$) in 2-day-old neonatal or adult mice of the indicated genotypes **(D)** adult mice of the indicated genotypes upon 4 weeks of DOX diet treatment. Lineage panel for splenic B: $Ter119^{-}CD11b^{-}Gr1^{-}CD3e^{-}$.

Figure S2

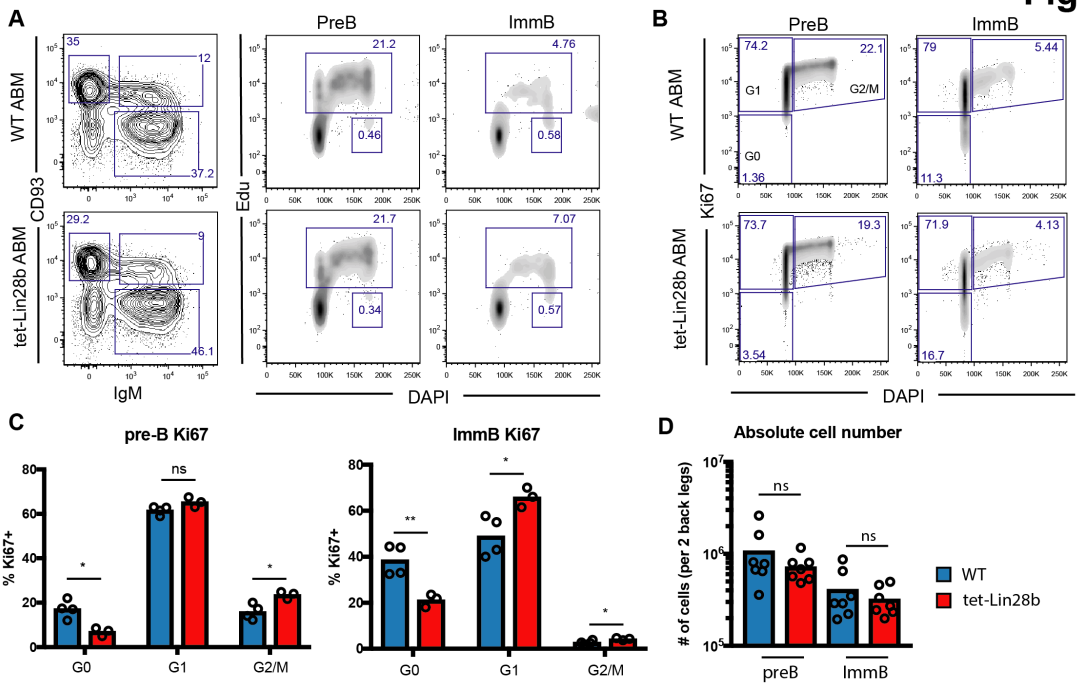

Figure S2; related to Figure 3

(A) Edu uptake FACS analysis of the indicated cell types 2 hours following one single intraperitoneal Edu injection from mice kept on a DOX diet for 4 weeks. **(B)** Cell cycle analysis using Ki-67 of the indicated cell types from mice kept on a DOX diet for 4 weeks. **(C)** Quantification of data in B. **(D)** Absolute cell numbers of the indicated populations per 2 back legs from mice kept on a DOX diet for 4 weeks. Data are obtained from 3 independent experiments. Significance was tested using a unpaired t-test. ns= not significant, *=P≤ 0.05.

Figure S3

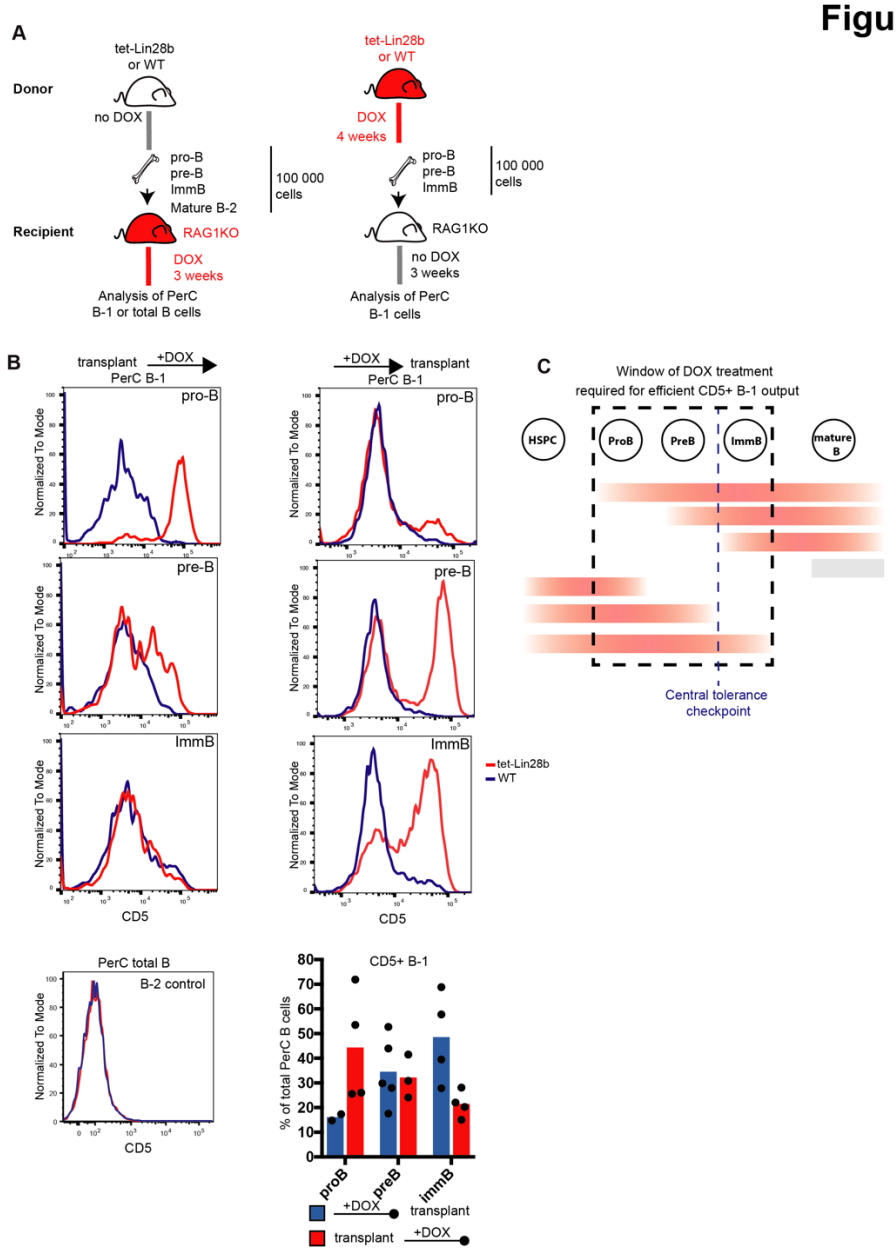

Figure S3; related to Figure 3

Determination of the DOX treatment window during B cell development required for efficient CD5+ B-1 cell output from tet-Lin28b ABM. (A) Schematic of adoptive transfer experimental set up. ProB cells were defined as: $Lin^{-}CD19^{+}IgM^{-}CD93^{+}CD43^{+}CD24^{lo}$, small pre-B cells as: $Lin^{-}CD19^{+}CD93^{+}IgM^{-}CD43^{-}CD24^{high}FSC^{low}$ and immature B cells as: $Lin^{-}CD19^{+}CD93^{+}IgM^{+}CD24^{high}$. $Lineage^{-}$: $Ter119^{-}CD11b^{-}Gr1^{-}CD3e^{-}$ **(B)** Readout of PerC B-1 cell CD5 expression of recipients adoptively transferred with the indicated cell types FACS sorted from the indicated donor sources with the indicated DOX treatment regimens at 3 weeks post transfer. **(C)** Schematic summarizing the data presented, indicating that DOX treatment between the pro-B and immB stages is required for robust $CD5^{+}$ B-1 cell output by tet-Lin28b ABM.

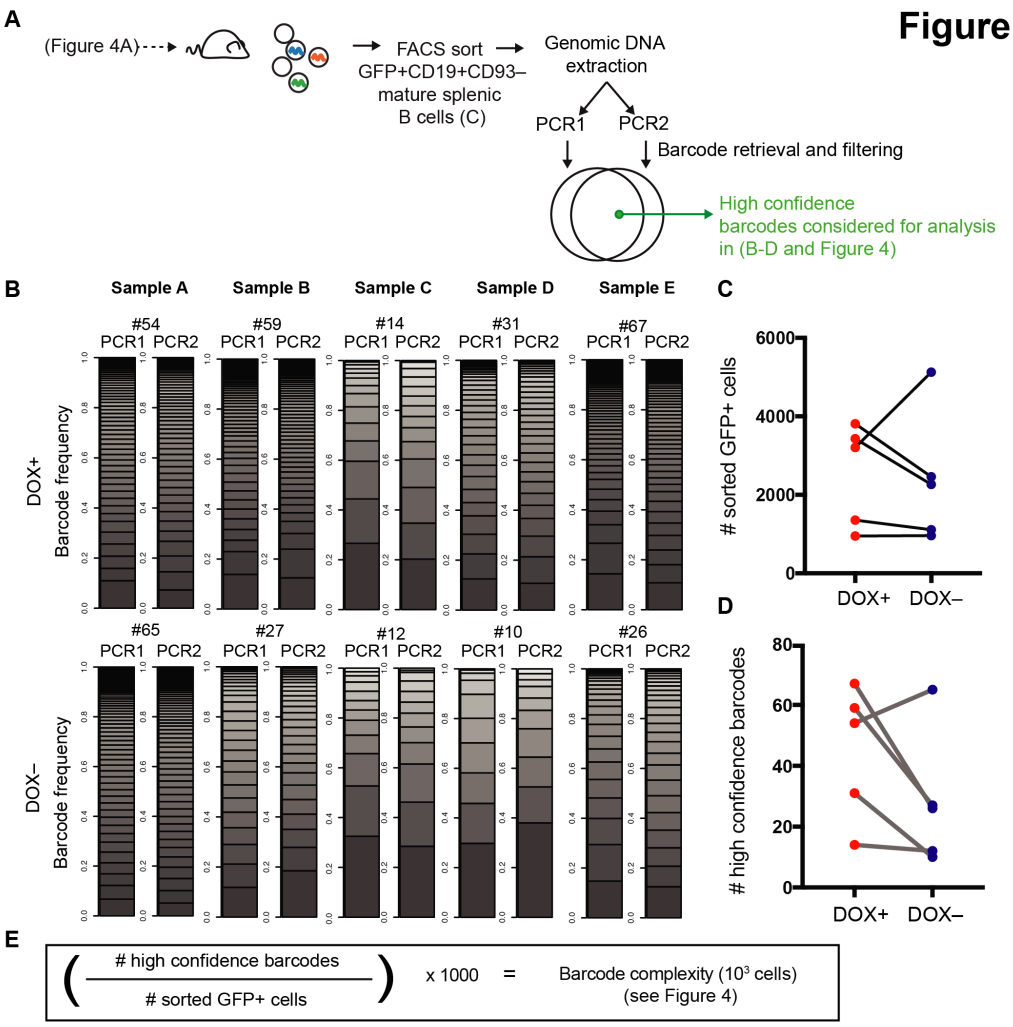

Figure S4; related to Figure 4

(A) Schematic of Barcode analysis strategy for data shown in Figure 4. **(B)** Stacked bar graphs represent read frequencies retrieved from the indicated populations by deep sequencing. Results from technical PCR replicates are shown side by side. Number on top of the bars indicate the number of unique high confidence barcodes detected in both replicates. **(C)** The absolute number of barcoded B cells sorted from recipients in Figure 4 by FACS. **(D)** The total number of unique high confidence barcodes detected. **(E)** Equation showing calculation used to enumerate barcode complexity in Figure 4C.

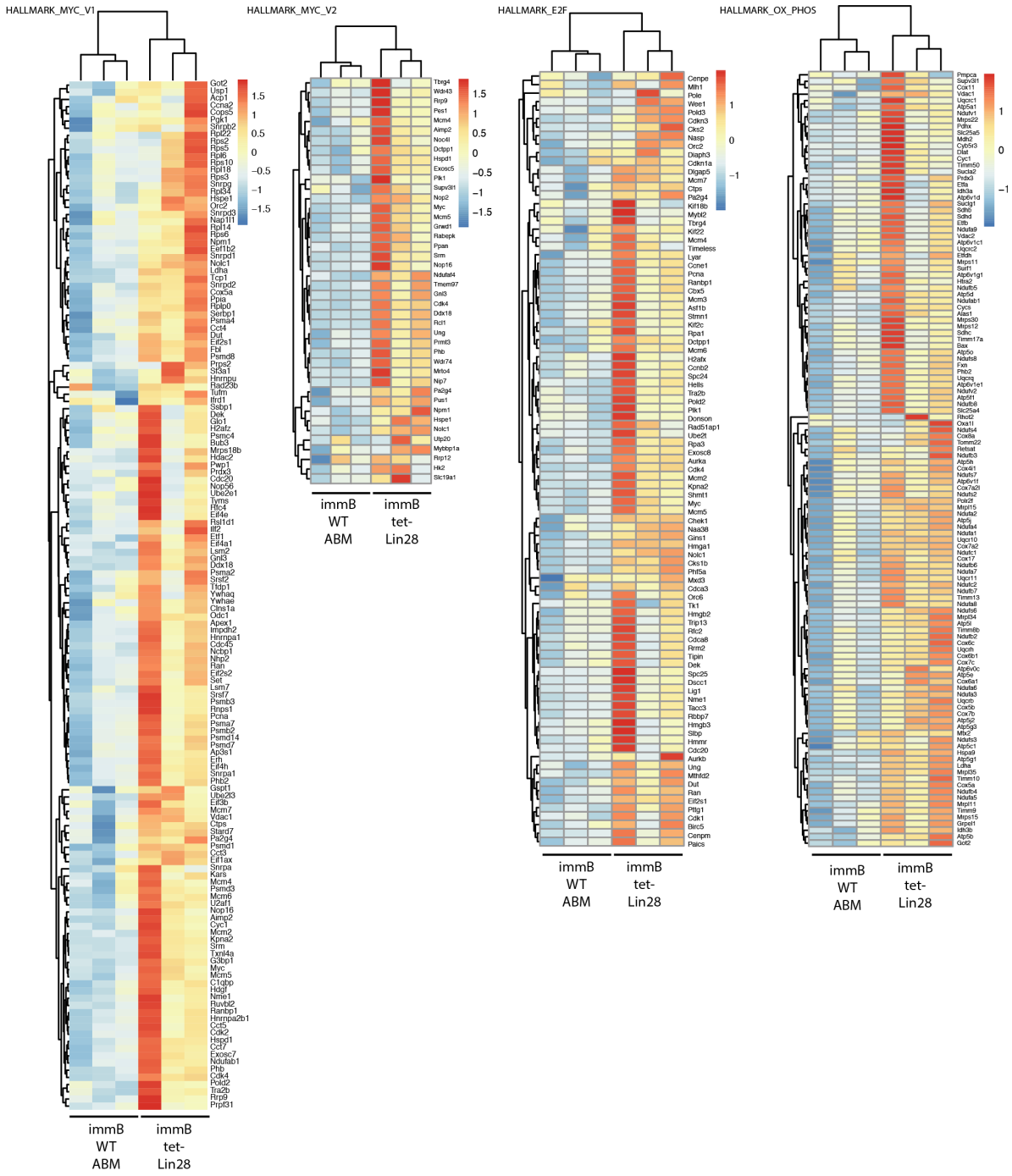

Figure S5

Figure S5; related to Figure 5

Heatmaps showing row z-scored expression values of genes in the indicated hallmark gene sets obtained from RNAseq of WT and tet-Lin28b immB cells on doxycycline food for 2weeks.

Figure S6

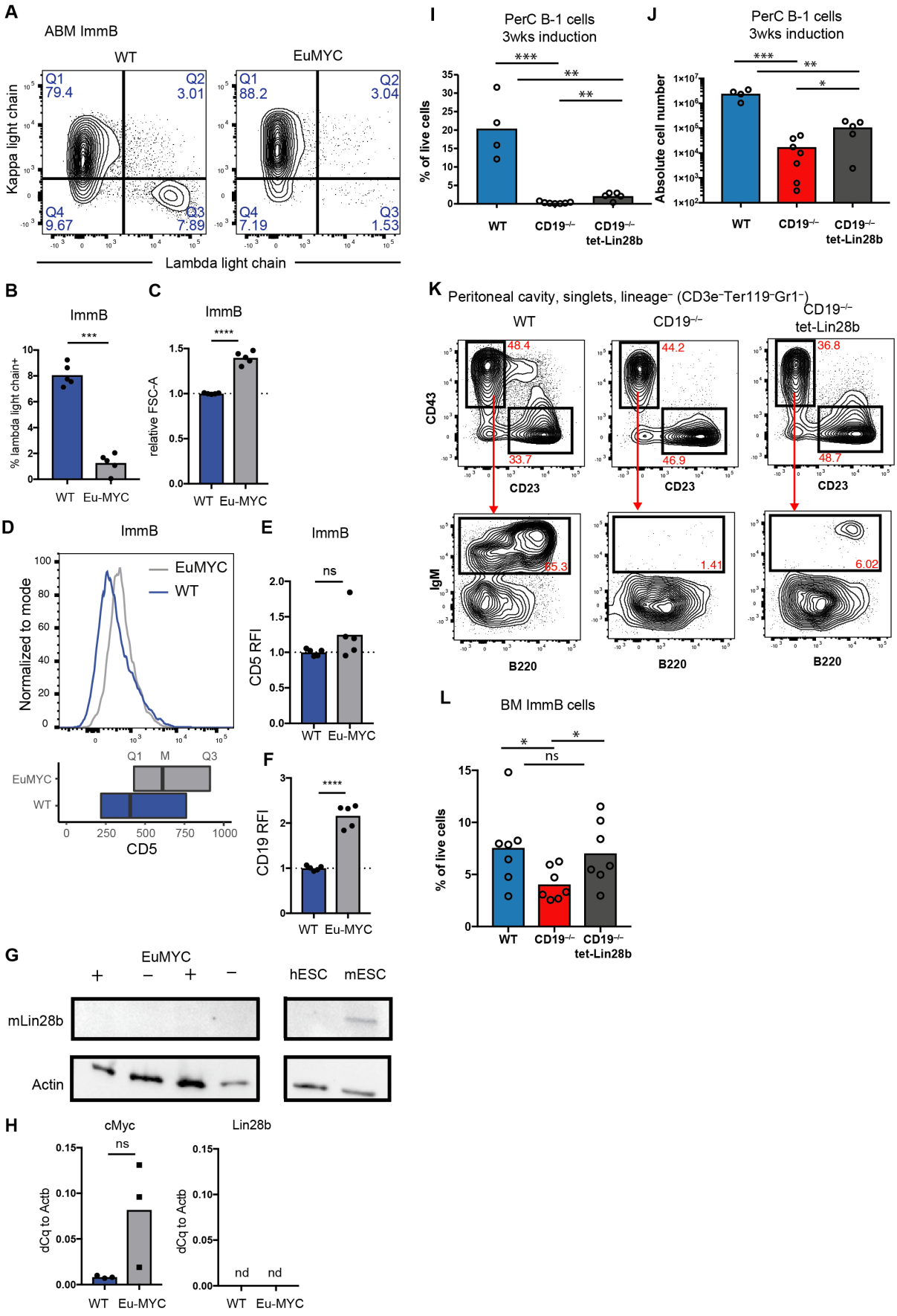
A
ABM ImmB
WT
EuMYC
Kappa light chain
Lambda light chain
Q1 79.4
Q2 3.01
Q4 9.67
Q3 7.89
Q1 88.2
Q2 3.04
Q4 7.19
Q3 1.53
B
ImmB
% lambda light chain+
WT Eu-MYC
C
ImmB
relative FSC-A
WT Eu-MYC
D
ImmB
Normalized to mode
EuMYC
WT
Q1 M Q3
CD5
E
ImmB
CD5 RFI
ns
WT Eu-MYC
F
CD19 RFI
WT Eu-MYC
G
EuMYC
hESC mESC
mLin28b
Actin
H
cMyc
Lin28b
dCq to Actb
ns
nd nd
WT Eu-MYC
I
PerC B-1 cells
3wks induction
% of live cells
WT CD19−/− CD19−/− tet-Lin28b
J
PerC B-1 cells
3wks induction
Absolute cell number
WT CD19−/− CD19−/− tet-Lin28b
K
Peritoneal cavity, singlets, lineage⁻ (CD3e⁻Ter119⁻Gr1⁻)
WT
CD19−/−
CD19−/− tet-Lin28b
CD43
CD23
IgM
B220
48.4
33.7
44.2
46.9
36.8
48.7
85.3
1.41
6.02
L
BM ImmB cells
% of live cells
ns
WT CD19−/− CD19−/− tet-Lin28b

Figure S6; related to Figure 6

(A) Representative FACS plots depicting Kappa and Lambda light chain usage in ABM ImmB cells of the indicated genotypes. **(B)** Quantification of data in A (n=5, from 2 independent experiments). **(C)** Quantification of relative FSC and **(D)** Histogram overlay depicting CD5 expression on ABM ImmB cells of the indicated genotypes. **(E)** Quantification of data shown in D (n=5, from 2 independent experiments). Data are shown relative to a representative WT sample in each experiment. **(F)** CD19 surface levels of ABM ImmB cells as determined by FACS. **(G)** Representative western blot showing murine Lin28b levels in lineage negative ($Ter119^{-}CD11b^{-}Gr1^{-}CD3e^{-}$) spleen cells from the indicated genotypes. Human ESC and murine ESC lysates were used as negative and positive controls for the antibody. **(H)** qPCR showing relative expression of cMyc and murine Lin28b in immature B cells of the indicated genotype. **(I)** Frequency and **(J)** absolute number of peritoneal cavity B-1 cells of mice with the indicated genotype, fed doxycycline food for 3 weeks. **(K)** Representative FACS plots of data in I. **(L)** Frequency of bone marrow immature B cells of mice with the indicated genotype, fed doxycycline food for 3 weeks (n=4-5, from 3 independent experiments). Significance was tested using an unpaired t-test. ns= not significant, ***=P≤ 0.001, ****=P≤ 0.001. nd= not detected.

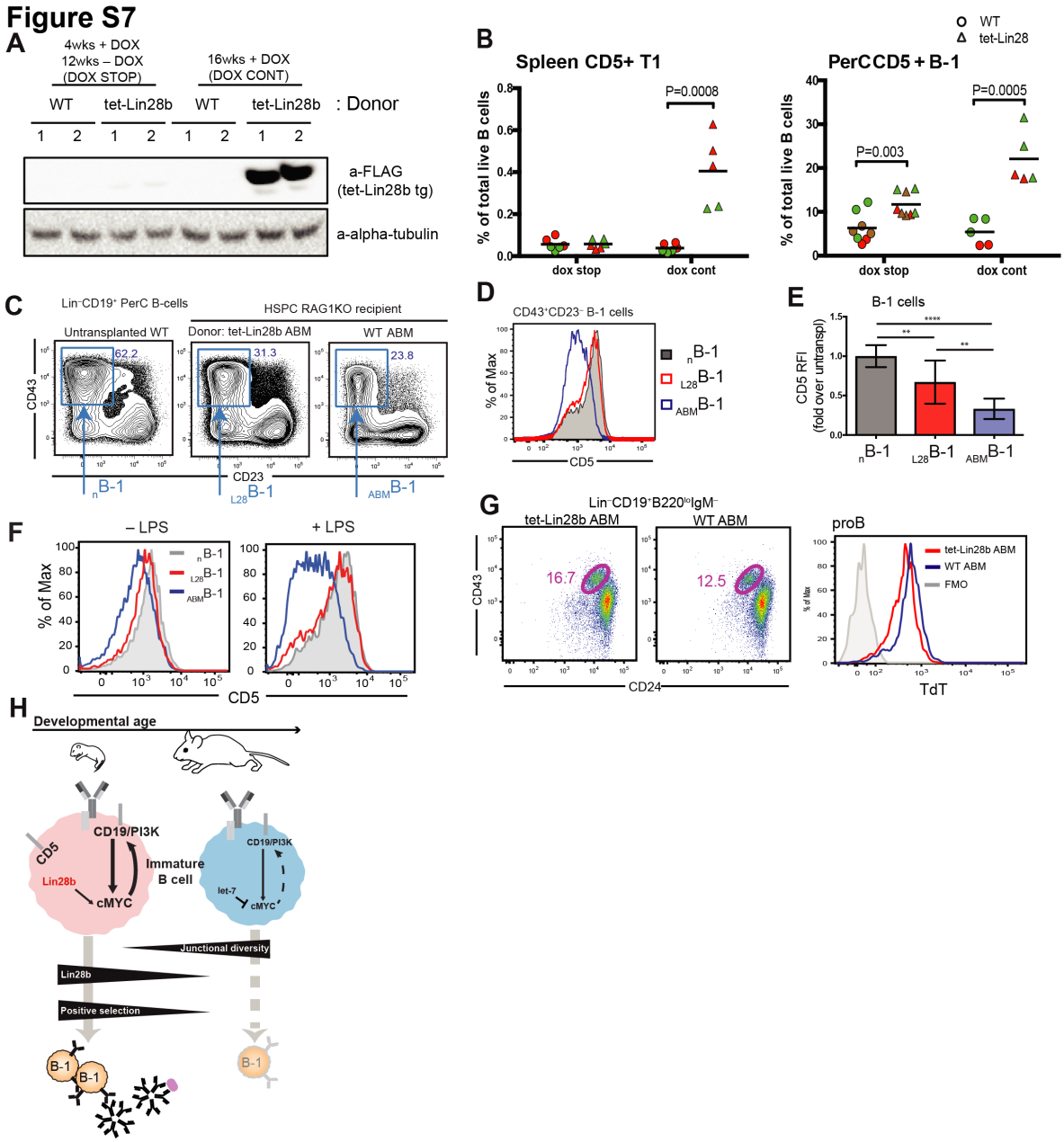

Figure S7; related to Figure 7

(A) (top) Western blot of lineage negative (Ter119$^-$CD11b$^-$Gr1$^-$CD3e$^-$) spleen cells depicting Lin28b transgene expression in Tet-Lin28b mice fed on a normal or doxycycline food diet for 4 weeks and WT mice fed doxycycline food for 4 weeks. (bottom) End-point western blot analysis for tet-Lin28b transgene expression in total splenocytes of recipient mice receiving the indicated DOX treatment regimens. Lysates from two representative recipient mice are shown for each condition. **(B)** Left panel: Frequency CD5$^+$ T1 B cells out of total splenic B cells from the indicated recipients as assessed by FACS. Right panel: Frequency of CD5$^+$ B-1 cells out of total peritoneal cavity B cells from the indicated recipients as assessed by FACS. Data points represent individual mice. Colors represent experimental replicates. **(C)** Representative FACS

analysis of donor derived B cells from Rag1KO recipient PerC at the endpoint of the DOX-STOP set-up (Figure 7A). **(D)** FACS analysis of CD5 levels of total B-1 populations gated in C. **(E)** Compilation of CD5 surface levels on total B-1 cells as gated in C. Levels are shown as the relative fluorescence intensity (RFI), when compared to control B-1 cells from an untransplanted WT adult mouse (n=6-14 biological replicates, from 3 independent experiments). **(F)** CD5 levels on the indicated populations following 36hr 10ug/ml LPS stimulation in vitro. **(G)** TdT levels in ABM pro-B cells from WT or tet-Lin28b mice fed DOX diet for 7 days. Where indicated, significance was tested using an unpaired t-test. Ns = not significant, *=P≤ 0.05, **=P≤ 0.01, ***=P≤ 0.001. Bars show the mean, error bars show the standard deviation of the mean.